Fall 2022

An Empirical Assessment of Environmental Variable Combinations for Use in Fire Weather Forecasts

Daniel Sunvold
San Jose State University

AN EMPIRICAL ASSESSMENT OF ENVIRONMENTAL VARIABLE COMBINATIONS FOR USE IN FIRE WEATHER FORECASTS

A Thesis

Presented to

The Faculty of the Department of Meteorology and Climate Science

San José State University

In Partial Fulfillment

of the Requirements for the Degree

Master of Science

by

Daniel Sunvold

December 2022

The Designated Thesis Committee Approves the Thesis Titled

AN EMPIRICAL ASSESSMENT OF ENVIRONMENTAL VARIABLE COMBINATIONS FOR USE IN FIRE WEATHER FORECASTS

by

Daniel Sunvold

APPROVED FOR THE DEPARTMENT OF METEOROLOGY AND CLIMATE SCIENCE

SAN JOSÉ STATE UNIVERSITY

December 2022

Craig Clements, Ph.D.	Department of Meteorology and Climate Science
Adam Kochanski, Ph.D.	Department of Meteorology and Climate Science
Patrick Brown, Ph.D.	Co-Director, Climate and Energy, The Breakthrough Institute, Berkeley, California

ABSTRACT

AN EMPIRICAL ASSESSMENT OF ENVIRONMENTAL VARIABLE COMBINATIONS FOR USE IN FIRE WEATHER FORECASTS

by Daniel Sunvold

Predicting high fire danger conditions is paramount to mitigating the impacts caused by wildfires. Such warning systems as red flag warnings (RFWs) and the National Fire Danger Rating System (NFDRS) utilize atmospheric and fuel moisture properties to warn public and government entities about conditions that may lead to the ignition or rapid growth of wildfires. In this study, we use high-resolution reanalysis and wildfire growth data from 2003-2020 in California to test a variety of different variables to determine if a more viable variable combination exists that could be used to create a better warning index which would allow for a better estimate of high fire danger conditions. This is assessed by ranking combinations based on how well they organize daily fire acreage growth values within the heatmaps. It is found that turbulent kinetic energy (TKE) 50 meters above ground level presents a strong case to be used as a fire danger predictor. Sounding profiles are also created to ascertain a clearer picture of the vertical profiles typically seen on dangerous fire weather days, with the highest average daily acreage growth values seen with each combination exhibiting a dry and warm-to-hot environment. Line plots detailing daily average acreage growth rate changes indicate compounding effects of multiple variables being in extreme states at the same time as well as limiting behavior where a single variable being in a non-fire conducive state can shut-off the influence of another variable. We also find that relative humidity and sustained wind speed is the third-ranked variable combination, empirically confirming a previous mostly heuristic result.

ACKNOWLEDGEMENTS

The work of this thesis could not be done without the help of many individuals. First and foremost, to Dr. Patrick Brown for his insight, guidance, encouragement, and patience over these past 18 months; without him, this work could not be done. To Dr. Craig Clements, for his tutelage over these past several months in the final stages of this work, and to Dr. Adam Kochanski, for his critique and help. Special thanks must also be given to them for anchoring my thesis committee. This work was possible due to funding provided by PG&E. I would also like to acknowledge Scott Strenfel and Dr. Richard Bagley for their advice and comments throughout the months of PG&E meetings with them.

My professors in both my undergraduate and graduate programs must be recognized, as well as the countless friends I made at both Virginia Tech and San José State University. Lastly, to my family. Sam, Savannah, and Kyle: thank you for your support and encouragement over these last two years. Grandma and Nana: thank you for indulging me by letting me talk your ears off about meteorology and fire weather. To my parents: thank you for your encouragement, support, and love, while also giving me a great deal on housing these past two years.

TABLE OF CONTENTS

LIST OF TABLES

LIST OF FIGURES

1. Introduction

Wildfires in California continue to worsen. The total annual area burned and average wildfire size continues to rise, while the wildfire season length has increased. Between 1984 and 2017, the total annual area burned in the state doubled (Dong et al. 2021). Forested regions in California have seen a particularly harsh increase in annual area burned, with a 766% increase in the summer months between 1972 and 2018 (Williams et al. 2019), though the annual area burned during the fall months has been found to have been increasing by around 40% per decade between 1984 and 2018 (Goss et al. 2020). The impacts of these wildfires are wide-ranging, from health issues due to poor air quality caused by smoke to economic and environmental losses. For example, within the Klamath Mountain forests of Northern California, non-native plant species have been introduced following severe wildfires, which could lead to ecological consequences (Reilly et al. 2020). Regarding the average wildfire size, the average decadal fire size across the Western United States has nearly tripled between the 1950s and 2010s (Weber and Yadav 2020). This can be seen clearly in recent wildfires across the state, with the top eight largest wildfires in California history transpiring since 2017, and all but two of the top twenty occurring since 2003 (CALFIRE 2022c). Both an increase in total area burned and the wildfire size also coincides with a prolonged wildfire season across the United States in general. In forested regions, the wildfire season length increased by 41% between 1979 and 2015 (Abatzoglou and Williams 2016), with significant trend increases in the length of the wildfire season found across much of the Western United States in general (Jolly et al. 2015).

Overall, the trends of increased annual area burned, wildfire size, and wildfire season length have led to an increase in severe consequences for local communities within California. This is particularly concerning when considering the wildland-urban interface (WUI), which marks the transition zone between undeveloped and developed land. Between 1970 and 2000, California was among the top 16 states that saw the greatest increase in the WUI (Theobald and Romme 2007). As of 2010, California had the most houses within the WUI (Martinuzzi et al. 2015), with half of the total buildings destroyed by wildfires in California between 1985 and 2013 occurring in this zone (Kramer et al. 2019). Thousands of structures have been burned, with entire communities such as Paradise and Greenville entirely incinerated. In the case of the Camp Fire of 2018, which destroyed Paradise, 85 people were killed and over 18,000 structures were destroyed, making this the most destructive wildfire in California state history (CALFIRE 2022a). Though the state has seen a great increase in the expansion of the WUI, it is still alarming that 15 of the top 20 most destructive wildfires in the state's history have occurred since 2015 (CALFIRE 2022d).

The impacts seen from wildfires can be expected to continue and worsen. A doubling of area burned is projected from 2010-2039 in the Sierra Nevada when compared to 1961-2004 (Kitzberger et al. 2017), while Yue et al. (2014) project that varying regions in Southern California would experience anywhere between 10-100% increase by the 2046-2065 time period. Additionally, model projections show a doubling of annual area burned in forested regions of the Western United States between 2021-2050 when compared to the historical period of 1991-2020 (Abatzoglou et al. 2021). Wildfire season length is also expected to continue to increase; for example, Ma et al. (2021) modeled that the wildfire season length in

the Santa Monica mountains (chaparral vegetation) could increase from anywhere between 5% and nearly 15% percent between 1960-1999 and 2080-2099. Considering this, it is imperative that scientists and operational meteorologists are using the most optimal environmental variables to predict destructive daily wildfire growth so that impacts can be lessoned. Forecasts such as red flag warnings (RFWs), the National Fire Danger Rating System (NFDRS), the Hot-Dry-Windy Index (HDW), and the Haines Index do not directly mitigate wildfires or their impacts, but they do lead to increased awareness of the fire danger, thus allowing for precautions to be taken that will allow for the mitigation of wildfires. Such precautions would include the banning of outdoor burning and the deployment of government resources to the areas most likely to see wildfire ignition or growth.

Several variables are currently utilized by meteorologists to dissect the potential fire danger on a given day. Primary variables used to present fire weather conditions include relative humidity, sustained wind speed, fuel moisture content, vapor pressure deficit (VPD), and temperature and are thus included in this study. As with any sector of meteorology, meteorologists predicting fire danger rely on more than one variable to create the best possible forecasts, with relative humidity and sustained wind speed remaining the primary variable combination used for the forecasting of fire weather throughout the public and private sectors, as they account for winds and moisture. The warning systems mentioned utilize a variety of the variables mentioned to compute their respective values.

National Weather Service meteorologists rely on sustained wind speed and relative humidity to determine if RFWs are warranted. Sustained wind speed can determine growth characteristics, with higher wind speeds amplifying the growth of wildfires (Abatzoglou et al.

2018; Keeley and Syphard 2019; Potter and McEvoy 2021). Thus, it is important to consider sustained wind speed when determining fire danger. Additionally, low relative humidity values aid in fire danger and fire growth. For example, recent research on wildfire activity in the Klamath Mountains of California shows that the severity of wildfires is high when the average relative humidity is below 35% (Estes et al. 2017).

The Haines Index is a simplistic value on a scale of one to six that describes the fire danger. This is done using air temperature and dew point temperature values at various levels of the lower atmosphere depending on geographical location. The HDW Index is composed of VPD and wind speed to describe the potential fire danger (Srock et al. 2018), while the NFDRS forecasts utilize fuel moisture content values, among other variables. The products noted represent a wide array of variables that may affect wildfire growth.

Using a combination of variables when forecasting fire danger allows for multiple meteorological factors to be accounted for that affect fire weather, thus increasing the accuracy of the forecasts. This is particularly important when issuing products like RFWs, with recent research having found that RFWs issued by National Weather Service offices in the Pacific Northwest have a high skill (Clark et al. 2020), but improvements can always be made. For example, Clark et al. (2020) notes that the performance rate of RFWs in the Pacific Northwest was higher for lightning-induced wildfires than human-induced ones, resulting in an area under which RFW forecast could be improved. Regarding NFDRS forecasts, fuel moisture content values are relied upon to make such forecasts; however, they use interpolated data and are not easily run, thus indicating another area in which fire forecasts can be improved. The benefits of the Haines Index have been scrutinized by several

voices within the wildfire community (Potter 2018; Srock et al. 2018), while the HDW index relies solely on atmospheric variable data and does not include fuel moisture data. The warning systems that have been developed provide vital information to meteorologists regarding the forecasting of fire weather danger, with improvements allowing for more precise forecasts to be developed.

The overall main purpose of this study is to determine what variable combinations using a variety of candidates best represent the daily danger represented by the acreage growth of wildfires. As mentioned, wildfire danger warning systems use a variety of variables, both meteorological and fuel related. Both types, as well as topographical variables, are used in this study so as to consider variable combinations that are not solely relied upon on variable type. Related to this is the desire to determine the general characteristics of the average daily acreage growth rates as the variable combination values change. Additionally, ascertaining knowledge of the average vertical profile soundings seen with specific variable combination values is a purpose of this study as well. Using average daily acreage growth as the primary fire variable is important for a multitude of reasons, such as the difficulty faced by firefighters and other government agencies to respond to and mitigate the impacts of wildfires when rapid growth rates are seen.

Table 1 shows the candidate variables used in this study, as well as their units and the specific variable type (surface meteorological, vertical profile meteorological, or topographic). The variables utilized in this study were chosen because of their inclusion in developed and currently operational products used by the National Weather Service and other government agencies and their noted impact on wildfire growth, with many of these

TABLE 1. Variables utilized in this study, the units of the variables, and the type of variable (surface meteorological, vertical profile meteorological, or topographic).

Variables Tested	*Units*	*Variable Type*
Daily mean Temperature	°C	Surface Meteorological
Daily mean Relative Humidity (RH)	%	Surface Meteorological
Daily mean Vapor Pressure Deficit (VPD)	kPa	Surface Meteorological
Fuel Moisture Content – DFM 100-hour	%	Fuel
Fuel Moisture Content – DFM 1000-hour	%	Fuel
Daily mean Sustained Wind Speed	mph	Surface Meteorological
Mean Precipitation Past 125 Days	mm/day	Surface Meteorological
Daily mean Saturation Vapor Pressure	kPa	Surface Meteorological
Daily mean Vapor Pressure	kPa	Surface Meteorological
Slope	%	Topographic
Aspect	degrees	Topographic
Elevation	meters	Topographic
Daily mean Planetary Boundary Layer Height	meters above ground level (AGL)	Vertical Profile Meteorological
Daily mean Haines Index	n/a	Vertical Profile Meteorological
Daily mean Horizontal Wind Speed 300 meters AGL	mph	Vertical Profile Meteorological
Daily mean Vertical Wind Speed 300 meters AGL	mph	Vertical Profile Meteorological
Daily mean Turbulent Kinetic Energy (TKE) 50 meters AGL	$m^2 s^{-2}$	Vertical Profile Meteorological

candidate variables changing due to anthropogenic climate change. As these trends are realized, the issuance of products such as RFWs and the NFDRS will be crucial to help prevent potential wildfire growth. Numerous studies have noted these trends over the past several years, as well as their effects on other variables.

Fuel moisture content – a key component of fire weather regimes that measures the amount of moisture in vegetation – is expected to decrease. In this study, dead fuel moisture (DFM) 100- and 1000-hour content values are used; these correspond to differing vegetation radii of one to three inches and three to eight inches, respectively, and the time lag needed for the difference in initial moisture content and equilibrium moisture content to reach 63% for a fuel particle. Globally, fuel moisture content has been found to be declining over the past several decades (Ellis et al. 2022). Within the Western United States, projections indicate that DFM 100-hour values will decrease across much of the region in the coming decades; however, there is disagreement regarding this trend among areas within California (Gergel et al. 2017). Decreasing fuel moisture is important to watch, as fuel moisture has been found to

have a significant relationship with fire activity, with long periods of low fuel moisture increasing fire activity (Abatzoglou and Kolden 2013). Regardless of the overall projections of DFM in California, fuel moisture itself is affected by such variables as temperature, which is expected to continue to rise as we progress into the 21st Century. It has been found that these warming temperatures will result in the fuel moisture components for various fuel types (surface, duff, and deep organic soils) becoming drier, with a needed corresponding increase in precipitation (15%, 10%, and 5% increase for each of the fuels mentioned for each degree increase in warming) to offset this trend (Flannigan et al. 2016).

Rising temperatures over the past several decades have already been realized, as decadal temperature increases of 0.3°C during the autumn months have been found between 1979 and 2018 (Goss et al. 2020). This coincides with research that states that temperature accounts for 40.4% of global grid cells that saw a significant increase in Fire Weather Index days that met the 95th percentile, thus helping to drive increases in extreme fire weather (Jain et al. 2022). Additionally, Williams et al. (2019) found that daytime temperatures during the March-October timeframe have increased by 1.4°C since the 1970s. Thus, these rises in temperature would aid in the decrease of fuel moisture content values. Rising temperatures also have noticeable effects on VPD. VPD, which represents the difference in the amount of moisture currently in the air and how much moisture the air can hold when saturated, is increased by rising temperatures through an increase in saturation vapor pressure. Williams et al. (2019) found that 78% of the increase in forested area burned during the summer months in California between 1972 and 2018 can be explained by the increase in VPD during the same time period. Significant positive trends between 1979 and 2020 in the days that met the 95th

VPD percentile criteria occurred in over 45% of the burnable area globally (Jain et al. 2022). Concurrently, the evaluation of multiple climate datasets has noted an increase in VPD since the 1990s (Yuan et al. 2019).

As mentioned, relative humidity, sustained wind speed (some minutes average), fuel moisture content, VPD, and temperature are primary variables used to present current fire weather conditions, with relative humidity and sustained wind speed remaining the primary variable combination used by meteorologists. Here, the RFW matrix currently in use by the National Weather Service will be tested using 2kmx2km resolution reanalysis and satellite-derived fire growth data from 2003 to 2020 in much of California to determine if its conventional variable combination (sustained wind speed and relative humidity) is optimal in terms of predictive power for extreme wildfire danger, with 136 unique pairwise variable combinations tested to determine the most optimal combination.

It is also important to understand how average daily acreage growth rates vary as variable values shift. Corresponding line plots detailing how average daily acreage growth values change based on the percentile values used are created in association with the heatmaps. The line plots indicate that the average daily acreage growth rates are nonlinear, which illustrates that the most extreme variable values can lead to disproportionately high acreage growth rates – something that is not readily communicated in the traditional RFW matrix. Finally, sounding profiles are created for each bin within the individual heatmaps (matrices). The soundings are created to investigate the vertical profiles of temperature, dew point, and wind in order to gain a more complete physical understanding of why different surface variable combinations are associated with different levels of daily fire growth. Most studies focus on

surface variables, but fire growth is also heavily influenced by the vertical structure of the atmosphere – especially stability and momentum aloft that can be transmitted to the surface. Vertical profiles are used in the computation of the Haines Index, so exploring the created soundings is sensible in this regard.

2. Data and Methods

The data utilized in this study contains a variety of different variables and corresponding values for each fire day at its respective location between 1 January 2003 and 31 December 2020. The reanalysis variables within the dataset include all variables except for relative humidity, saturation vapor pressure, and vapor pressure. Those three variables were calculated based on the reanalysis variables in the dataset. Temperature was converted from units of Kelvin to units of degrees Celsius, while the three wind variables (sustained wind speed, horizontal wind speed 300 meters above ground level (AGL), and vertical wind speed 300 meters AGL) were converted from meters per second to miles per hour; this was done to convert the units into those more familiar to the operational meteorological community and the public.

Daily fire growth statistics for each day within the time period were calculated by Sonoma Technology (https://www.sonomatech.com/) utilizing data collected by NASA's Terra and Aqua satellites MODIS system. The National Center for Atmospheric Research's Weather Research and Forecasting (WRF) model (version 4.1.2) provided the dataset reanalysis variables at an hourly rate at a high resolution (2km by 2km). Initial and boundary conditions for the WRF reanalysis were provided by the National Centers for Environmental Prediction's Climate Forecast System Reanalysis (CFSR), with CFSR being used for all data from 2003 to 2011 and CFSv2 being used for all data after 2011. Nested domains were utilized in the reanalysis, with grid resolutions of 18, 6, and 2 kilometers. Parameterizations used were as followed: 20mb for model top pressure level; MODIS30s with lakes for land use; NoahMP for land surface model; RRTMG for radiation schemes; Thompson for

microphysics scheme; MYNN2.5 for planetary boundary layer scheme; MYNN for surface layer scheme; Kain-Fritsch for the cumulus scheme in the outer domain; topographic shading and slope-dependent radiation for the innermost domain. There was a total of 50 vertical levels. Although the WRF reanalysis dataset provided was initially at an hourly time scale resolution, the variables were averaged to a daily time scale resolution to coincide with the daily time scale resolution of the fire growth data. This amounted to 17,910 individual fire days and 8,633 individual fires and their daily growth and meteorological, fuel, and topographical reanalysis values making up the dataset.

The fuel moisture content variables were calculated at 100-hour and 1000-hour levels. This was done by integrating the following ordinary equation, Equation 1, over a time period of 3,000 hours preceding the individual fire:

$$\frac{dm}{dt} = \frac{E - m}{t_L}$$

The following ordinary equation, Equation 2, is used to amend the equilibrium value so as to collect an accurate picture of the starting moisture content conditions:

$$\frac{dm}{dt} = \begin{cases} \frac{E_d - m}{t_L} \; if \; m > \; E_d \\ 0 \; if \; E_d \geq m \; \geq \; E_w \\ \frac{E_w - m}{t_L} \; if \; m < \; E_w \\ \frac{S - m}{T_r}\left(1 - e^{\frac{r - r_0}{r_s}}\right) if \; r > \; r_0 \end{cases}$$

with E_d and E_w represent the drying and wetting equilibrium, respectively. The last condition in ordinary differential equation is utilized when it rains. E_d and E_w are represented by the following equations, Equation 3 and Equation 4:

$$E_d(T) = 0.924 * RH(T)^{0.679} + 0.000499 * e^{0.1*RH(T)} + 0.18 * (21.1 + 273.15 - T)(1 - e^{-0.115*RH(T)})$$

$$E_w(T) = 0.618 * RH(T)^{0.753} + 0.000454 * e^{0.1*RH(T)} + 0.18 * (21.1 + 273.15 - T)(1 - e^{-0.115*RH(T)})$$

Using these equations, the DFM 100- and 1000-hour values within the dataset.

The provided dataset defines the study area, with portions of Southern California not included, as it was excluded from the two-kilometer resolution domain of the WRF reanalysis. As such, the southern boundary of the study area is 33.6042°N, which is roughly equal in latitude to Laguna Beach, CA. The eastern portion of the study area boundary is 116.752°W, which runs east of the San Bernardino and Inyo National Forests in California. All areas north and west of those boundaries are included in the study area, with the northern boundary being the Oregon-California state border. The general location of all the individual fires included in the dataset used can be seen in Figure 1.

As mentioned, the values for the variables utilized represent a daily average for each individual fire growth day. The date, fire identification number, daily acreage growth rate, and longitude and latitude coordinates of each fire represent the daily fire statistics, calculated using NASA's MODIS system. The reanalysis weather variables include mean daily temperature (°C), mean daily VPD, mean precipitation in the past 125 days (mm/day), and mean daily wind speed (mph). DFM in the 100- and 1000-hour intervals (DFM 100-hour and DFM 1000-hour) represent the fuel moisture content portion of the dataset. Topographic variables include slope, aspect (orientation of the surface), and elevation. Vertical profile variables consist of horizontal and vertical wind speed 300 meters AGL, turbulent kinetic energy (TKE) 50 meters AGL, and the planetary boundary layer height. The Haines Index value for each individual fire on each day is also included in the dataset. Saturation vapor

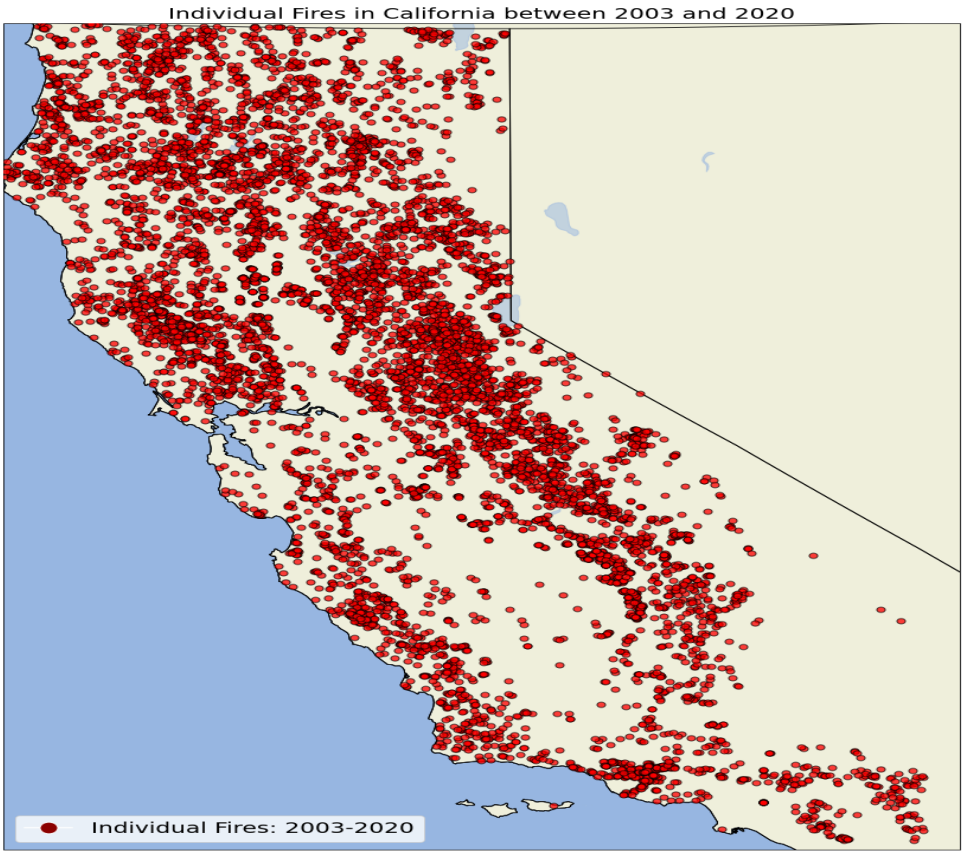

FIG. 1. Individual fires within much of California between 2003 and 2020. Each red dot represents a specific fire, with 8,633 different fires over the period of the dataset (1/1/2003 – 12/31/2020).

pressure and vapor pressure – two of the aforementioned calculated variables – are used to derive relative humidity. Land use type was also included in the dataset using nine different categories defined by WRF; these were then resolved to three land types: forest (1), shrub (2), and savanna and grassland (3). This totals to 25 different variables within the dataset, representing WRF reanalysis output variables, calculated variables, and MODIS fire detection data. It should be noted that there are various fire day values missing for the vertical profile variables, which has the potential effect of diluting the data. This is likely because of missing sounding profiles taken on those days.

Of the 25 variables within the dataset, 17 are used as candidate variables for this study, shown in Table 1. The 14 variables that are of the meteorological or fuel type are space and time-varying variables, changing daily. The remaining three variables (aspect, topography, elevation) are space-only-varying variables, varying by location within the study area. Each variable is matched to other 16 variables, resulting in 136 unique pairwise variable combinations in total. This enables every possible combination to be tested, including combinations between the time- and space-varying variables. We systematically investigate how well each pairwise variable combination describes daily wildfire growth in an effort to test whether the variables traditionally used in the RFW system are indeed the most useful. The variables must be normalized in order to compare them on a standard scale, so percentiles (5^{th}, 25^{th}, 50^{th}, 75^{th}, and 95^{th}) are found for each of the 17 variables used where percentiles are calculated on variable values at fire locations not over the entire domain.

A forced correction is done on the percentile values for the Haines Index; while the Haines Index value for a given fire day is not necessarily a round value within the range of possible Haines Index values (2-6), the 95^{th} Percentile value initially calculated corresponds to the value of 6 – the highest possible Haines Index value. This is changed as the 95^{th} Percentile cannot be the highest possible value; therefore, it was forcibly lowered to a 5.99 value. Each individual fire day and their 17 observed and calculated variables are then categorized into six specific bins (<5th Percentile, 5th-25th Percentile, 25th-50th Percentile, 50th-75th Percentile, 75th-95th Percentile, >95th Percentile) and matched with the bins of their corresponding variable combinations.

Pivot tables are created that aggregate the average daily acreage growth values for each bin combination within each variable combination (i.e., <5th Percentile Variable A and 25th-50th Percentile Variable B), resulting in 36 values being calculated. Following this, heatmaps displaying the average daily acreage growth for each of the 36 bins of each variable combination are created. The idea is that if a given variable combination is useful for predicting daily wildfire growth, then observed growth should change more-or-less monotonically with joint changes in the variables. Additional heatmaps displaying the number of fire days each bin criteria met are also created, allowing for a determination to be made on if the average daily acreage growth values can be trusted based on the number of fire days used in each calculation (around 25-30 days minimum).

136 heatmaps (6-by-6 matrices) displaying the average daily acreage growth rates are created. The heatmaps add historical context by providing the average daily acreage growth values that met specific variable percentile values. This creates a reference system that allows for future general estimations of the average daily acreage growth rates that may be seen on a given day that meets the variable combination percentile values. The ranking system incorporates value trends in the columns, rows, and diagonals of the heatmap, and values a convergence of the average daily acreage growth values to a corner. For example, a heatmap with values converging to the top-left corner (bin) would have its column values increase from bottom to top, its row values increase from right to left, its diagonal values increase from bottom-right to top-left, and its highest average daily acreage growth value occupying the top-left corner. This convergence is desired, as the corresponding corner percentiles represent the variable values that would lead to the most significant fire danger. Thus, having

this convergence would affirm accepted ideas regarding conditions leading to dangerous fire conditions (i.e., low relative humidity and high wind speeds leading to explosive growth).

The ranking system is designed to check each corner of the heatmap for the convergence of average daily acreage growth rates. A value of one is given to each column, row, and diagonal bin that increases in value. If a bin increase is followed by a bin decrease, and then followed by another bin increase, values of one, zero, and one would be assigned, respectively. The beginning bins in each row, column, and diagonal furthest from the corner being studied are not considered, as there is no prior value to base an increase or decrease on; in the example noted above, the bottommost column bins, rightmost row bins, and the bottom-right diagonal bin would not be considered and thus assigned a value of zero. The values are then summed, with an added value of three assigned if the highest average daily acreage growth value occupies the corner the values are converging towards. This added weight is included to emphasize the importance of the highest average daily acreage growth rate occupying one of the four corners. The highest possible value is 68, with no variable combinations in this study reaching that value. Heatmaps are not discriminated against regarding which corner they converge to; as mentioned, the system created accounts for convergence to either of the four corners, checking each one and selecting the convergence that has the highest sum value. A list containing the total summed value for each heatmap is then created. The scoring system rules are shown in Table 2.

An example heatmap is shown in Table 3. The values from the heatmap rows and columns are extracted and plotted – hereafter referred to as line plots. Two line plots are created for each variable combination, with the average daily acreage growth rates

TABLE 2. The rules for the ranking system.

Ranking Rules
The first bin of the row, column, and diagonal furthest from the corner being considered is assigned a value of 0 because of no prior average daily acreage growth value to base it off.
If each subsequent bin in each row, column, and diagonal sees an increase in average acreage value, a value of 1 is assigned.
If a bin increase is followed by a bin decrease, the bin with the decreased value is assigned a value of 0.
If the highest acreage growth value is in one of the four corners of the matrix, an added value of 3 is assigned. Ideally, the corner bin would have the highest acreage growth value, but this is not always the case.
Because value convergence can occur at one of four corners, the system is designed to check all possible combinations of the row, column, and diagonal reads (i.e., left to right, bottom to top, etc.) and the highest possible summed value will be taken. This ensures that the ranking system accurately ranks the heatmaps and does not disregard any possible convergence.
The highest possible score value is 68.

representing the y-axis. For each line plot, one of the variable's percentile bins within the combination being considered is used as the x-axis, while the other variable's percentile bins are plotted individually. The objective of these plots is to extract general characteristics regarding the change in the average daily acreage growth rates as the variable values change, thus gaining insight into how the variable combination values influence the growth rates.

Vertical profile data that contains various variables such as temperature, dewpoint temperature, pressure, and u and v wind values are used to create sounding profiles for the highest average daily acreage corner bin and opposite corner bin in the individual heatmaps. This vertical profile data aligns with the fire dataset referenced previously, thus allowing for the matching vertical profile data to be selected for every fire day in each bin. The soundings are plotted with air temperature, dewpoint temperature, parcel profile, and wind barbs. The vertical profile data is averaged for each bin using the fire days that met the criteria of the bin. The standard dry adiabats, moist adiabats, and mixing ratio lines are plotted on the

TABLE 3. A heatmap mockup. The plot shows simulated average daily acreage growth rates (in acres), as well as the ranking system for it. The three numbers below the average daily acreage growth rate represent the three different methods for determining the total value of the heatmap. The values are then summed.

9547 Acres $1^{Diagonal}$ 1^{Column} 1^{Row} $3^{Highest\ Value}$	**6623 Acres** 1^{Column} 1^{Row}	**2005 Acres** 0^{Column} 1^{Row}	**1250 Acres** 1^{Column} 1^{Row}	**798 Acres** 1^{Column} 1^{Row}	**425 Acres** 1^{Column} 0^{Row}
7652 Acres 1^{Column} 1^{Row}	**5571 Acres** $1^{Diagonal}$ 1^{Column} 1^{Row}	**2069 Acres** 1^{Column} 1^{Row}	**1101 Acres** 1^{Column} 1^{Row}	**731 Acres** 1^{Column} 1^{Row}	**402 Acres** 1^{Column} 0^{Row}
3100 Acres 1^{Column} 1^{Row}	**2551 Acres** 1^{Column} 1^{Row}	**1614 Acres** $1^{Diagonal}$ 1^{Column} 1^{Row}	**897 Acres** 0^{Column} 1^{Row}	**683 Acres** 1^{Column} 1^{Row}	**377 Acres** 1^{Column} 0^{Row}
1341 Acres 1^{Column} 1^{Row}	**1114 Acres** 1^{Column} 1^{Row}	**865 Acres** 1^{Column} 0^{Row}	**907 Acres** $1^{Diagonal}$ 1^{Column} 1^{Row}	**505 Acres** 0^{Column} 1^{Row}	**325 Acres** 1^{Column} 0^{Row}
755 Acres 1^{Column} 0^{Row}	**765 Acres** 1^{Column} 1^{Row}	**712 Acres** 1^{Column} 1^{Row}	**505 Acres** 1^{Column} 0^{Row}	**525 Acres** $1^{Diagonal}$ 1^{Column} 1^{Row}	**207 Acres** 0^{Column} 0^{Row}
406 Acres 0^{Column} 0^{Row}	**425 Acres** 0^{Column} 1^{Row}	**398 Acres** 0^{Column} 1^{Row}	**331 Acres** 0^{Column} 1^{Row}	**298 Acres** 0^{Column} 1^{Row}	**267 Acres** $0^{Diagonal}$ 0^{Column} 0^{Row}

soundings. The lowest pressure possibly plotted varies by variable combination but is around 20 millibars for each combination; however, for simplicity, all data points below 100 millibars are disregarded.

3. Results and Discussions

a. Heatmap results

For simplicity, the paper will focus on five of the top six ranked heatmaps and their related soundings, as well as notable variable combinations throughout the rankings. The one exception within the top six that will not be discussed or shown is sustained wind speed and DFM 1000-hour; the reason for this is the physical and visual similarities between DFM 100-hour and DFM 1000-hour. By focusing on five of the top six, the most optimal variable combinations will be presented, allowing for more focus to be given to these combinations. The top six variable combinations (including sustained wind speed and DFM 1000-hour) by summed value are shown in Table 4.

TABLE 4. The top five variable combination rankings are shown here. The total score (out of 68 possible points) and the score percentage ($\frac{\text{score}}{68} * 100$) are also shown. The corresponding figure number is included as a reference.

Ranking	***Variable Combination***	***Figure***	***Score (out of 68 possible points)***	***Score Percentage***
First	RH vs. TKE 50m	Fig. 2	60/68	88.23%
Second	Sustained WS vs. DFM 100-hour	Fig. 3	59/68	86.76%
Tied-Third	Sustained WS vs. DFM 1000-hour	N/A	57/68	83.82%
Tied-Third	Sustained WS vs. RH	Fig. 4	57/68	83.82%
Tied-Fifth	DFM 1000-hour vs. TKE 50m	Fig. 5	55/68	80.88%
Tied-Fifth	Vapor Pressure vs. TKE 50m	Fig. 6	55/68	80.88%

The following five figures are the resultant heatmaps for each of those variable combinations. The convergence of the average daily acreage growth values to a specific corner can clearly be seen with these heatmaps.

Perhaps the most surprising result of this study was the emergence of TKE 50 meters AGL as a viable variable in predicting large daily acreage growth of wildfires. TKE is defined as the amount of energy in turbulent eddies generated by wind shear and buoyancy

effects (Heilman and Bian 2010). Alternatively, TKE acts as a measure of the amount of kinetic energy within turbulent flows. Limited research has been done on the effects of TKE on wildfires, but it is not without precedence. Heilman and Bian (2010) have researched its effects – combined with the Haines Index – on wildfires within the Great Lakes and New England regions of the United States and noted that high wind gusts and variable wind regimes are associated with high TKE values near the surface. Therefore, high TKE values could aid in the production of volatile wildfire environments that lead to the explosive growth of wildfires because of the associated winds that accompany them, with fire growth being exacerbated further by dry conditions. In their study, Heilman and Bian (2010) found that over 37% of large wildfires that occurred in the New England and Great Lakes regions between 2005 and 2007 had near-surface TKE values in excess of 3 $m^2 s^{-2}$. In this study, the 95th percentile value for TKE 50 meters AGL was about 2.8 $m^2 s^{-2}$, closely mirroring Heilman and Bian's results. The TKE 50 meters AGL and relative humidity heatmap is shown in Fig. 2. TKE 50 meters AGL and relative humidity saw a total score of 60 out of 68, resulting in a score percentage of 88.2%. The highest average daily acreage growth values corresponded with relative humidity values that fell below 25% (25th percentile value).

Low relative humidity values being a driver in wildfire activity and wildfire danger falls in line with past research (Brey et al. 2018; Dong et al. 2021; Jain et al. 2022; Williams et al. 2019). However, it is surprising to see that, overall, in the top rankings, relative humidity outperforms VPD. This goes against recent work that establishes VPD as a prime moisture variable to use regarding potential area burned (Seager et al. 2015; Williams et al. 2015). 102 of the 17,871 fire days considered (TKE values were missing for 39 days) were categorized

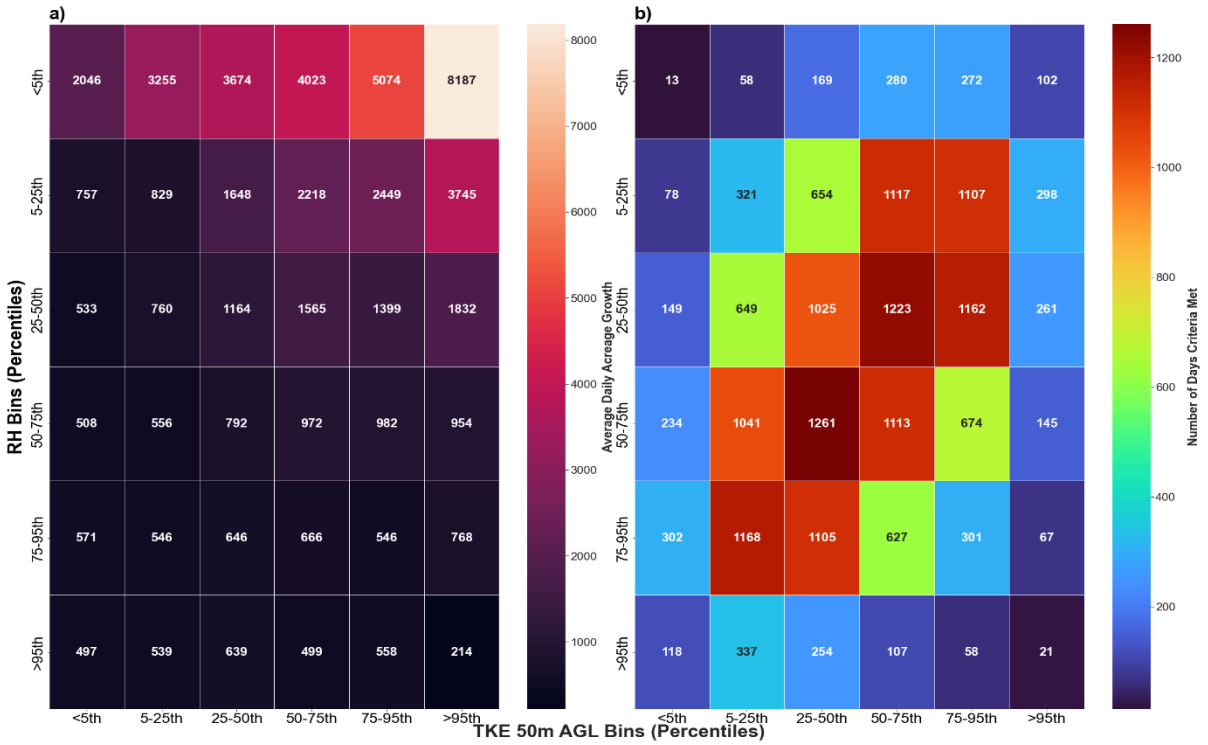

FIG. 2. The heatmap for Relative Humidity and TKE 50m AGL. In Fig. 2a, a convergence of values to the top-right corner can be seen in this heatmap, indicating a clear relationship between increasing average daily acreage growth and decreasing RH values and increasing TKE values. Fig. 2b shows the number of individual fire days that met the Relative Humidity and TKE 50m AGL criteria.

in the top-right bin (<5th Percentile RH, >95th Percentile TKE 50 meters AGL), resulting in a total summed-area burned of over 835,000 acres, representing the largest daily acreage growth average in the heatmap at 8,187 acres.

Much like with TKE 50 meters AGL, sustained wind speed appeared multiple times in the top rankings. This confirms its utility as a variable highly predictive of fire danger. Sustained wind speed and DFM 100-hour (Fig. 3) had a total score of 59 out of 68 - falling just below relative humidity and TKE - for a score percentage of 86.8%. Research has found that high wind speeds and low DFM 100-hour values coincide with large human-ignited wildfires across the Western United States, with nearly a third of the large wildfires

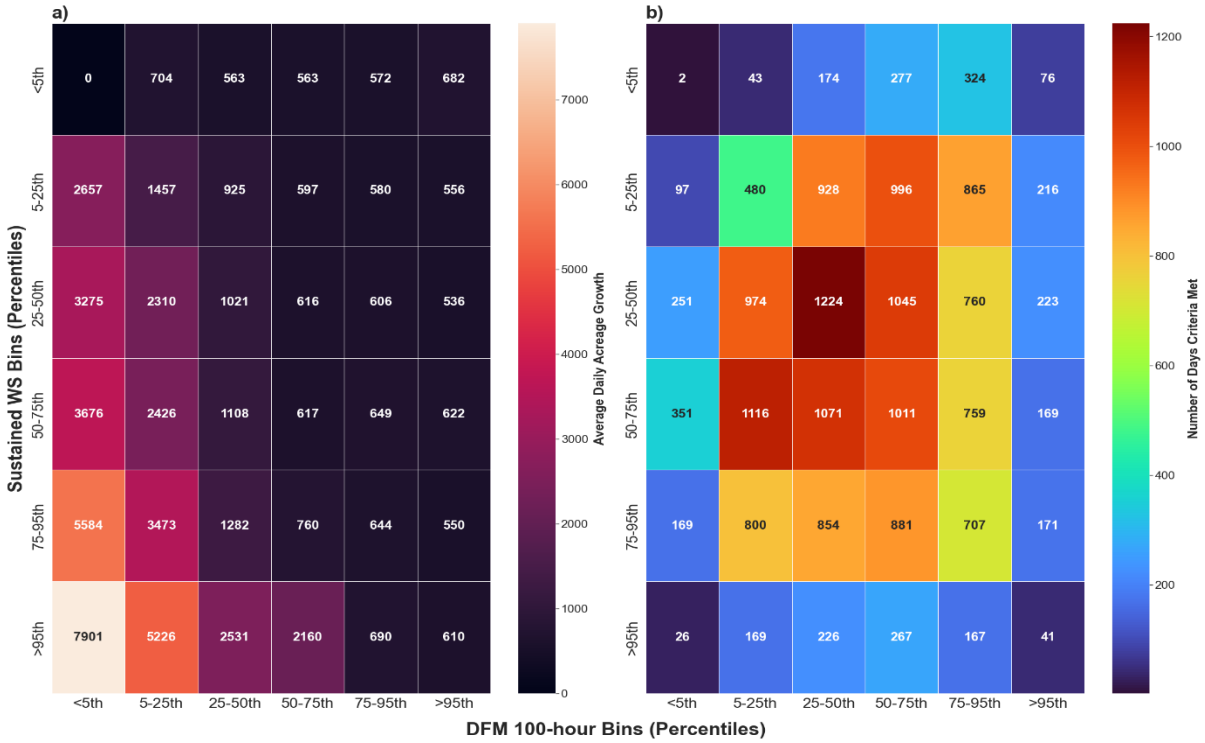

FIG. 3. The heatmap for Sustained Wind Speed and DFM 100-hour. In this case, a convergence to the bottom-right corner can clearly be seen in this heatmap (Fig. 3a).

coinciding with wind speeds above 5 m/s (11 mph) (Abatzoglou et al. 2018). Similar to the TKE values, this closely mirrors the corresponding sustained wind speed value for the highest average daily acreage growth rate in the heatmap, which is 10.7 mph, or just below 5 m/s. Sustained wind speed and DFM 1000-hour had a total score of 57 out of 68, for a score percentage of 83.8%, but will not be discussed further in this paper due to the similarities, both physically and visually, between sustained wind speed and DFM 1000-hour and sustained wind speed and DFM 100-hour, as previously mentioned.

The highest average acreage growth values for the sustained wind speed and DFM 100-hour combination occurred in the bottom-left bins of Figure 2 (<5th Percentile DFM 100, >95th Percentile sustained wind speed), corresponding to a DFM 100-hour value of less than 6.4%, with sustained wind speeds of 10.7 mph, as mentioned above. For sustained wind

speed and DFM 100-hour, 26 out of 17,910 fire days were categorized in the bottom-left bin, resulting in a total summed-area burned of over 205,000 acres, with an average of 7,901 acres burned per day. Sustained wind speed and DFM 1000-hour saw 34 out of 17,910 fire days categorized in the bottom-left bin for an average of 5,901 acres burned daily and a total summed-area burned of over 200,000 acres.

The most common variable combination used to distribute fire danger information to the public, sustained wind speed and relative humidity (Fig. 4), tied for third in the rankings with sustained wind speed and DFM 1000-hour. Such combinations must be particularly monitored in Northern and Southern California, where Diablo and Santa Ana wind events occur, respectively. Like the sustained wind speed and DFM 100-hour combination, the highest daily acreage growth average occurred in the bottom-left bin of the heatmap. This corresponded to percentile values of less than 13.7% relative humidity (<5th Percentile) and the aforementioned wind speed values of greater than 10.7 miles per hour (>95th Percentile). 111 out of 17,910 fire days met these criteria, resulting in an average daily acreage growth value of 9,483 acres and a total summed acreage growth of over 1,000,000 acres.

DFM 1000-hour and TKE 50 meters AGL tied for fifth with vapor pressure and TKE 50 meters AGL. Both variable combinations had a total score of 55 out of 68, resulting in a percentage score of 80.9%. The values converged to the top-right portion of the heatmaps, with the top-right bin seeing the highest average daily acreage growth value at 9,664 acres for DFM 1000-hour and TKE 50 meters AGL (seen in Fig. 5), while vapor pressure and TKE 50 meters AGL had a highest average daily acreage growth value of 7,334 acres. These bins correspond to the greater than 95th percentile (values greater than 2.8 $m^2 s^{-2}$) for TKE 50

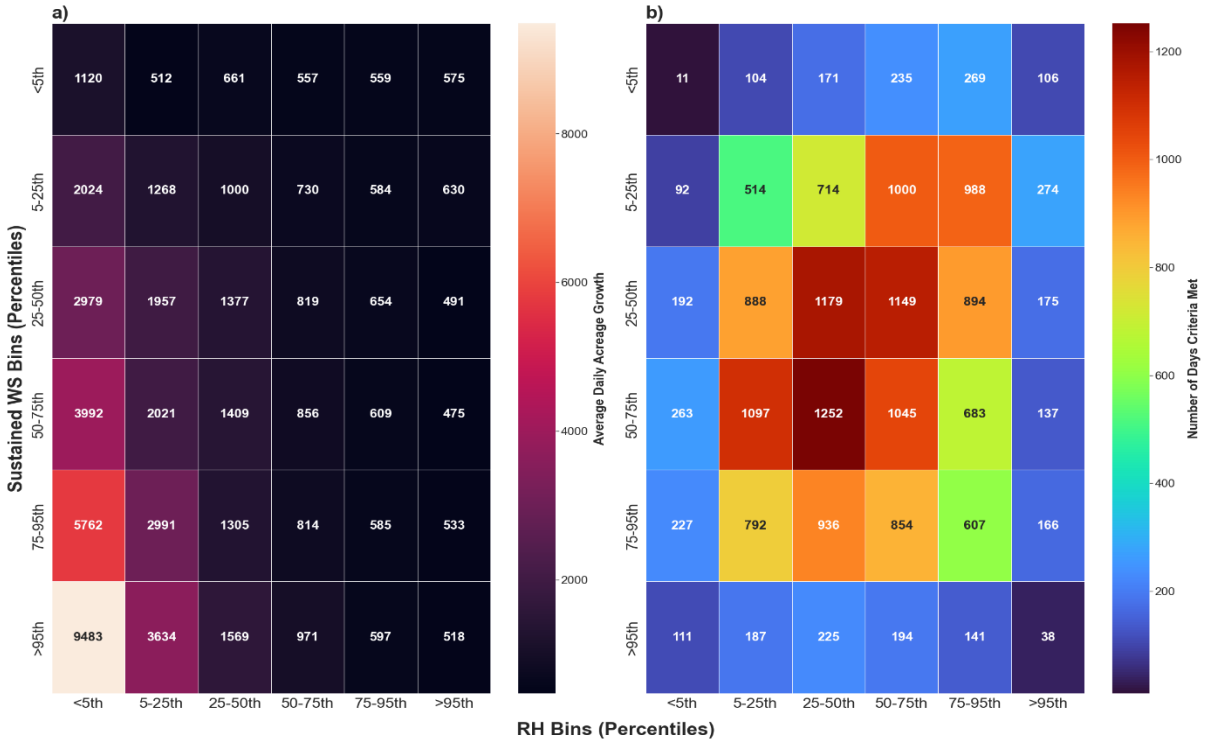

FIG. 4. The heatmap for Sustained Wind Speed and Relative Humidity. Another example of a strong convergence to a corner (bottom-right) can be seen in Fig. 4a, indicating another strong relationship between increasing average daily acreage growth values and decreasing Relative Humidity and increasing Sustained Wind Speed values.

meters AGL and less than 5th percentile for DFM 1000-hour (values less than 8.1%) and vapor pressure (values less than 0.26 kPa). The DFM 1000-hour 95th percentile value agrees with previous research done by Brey et al. (2018), who found that wildfires in Mediterranean California ecoregions that occurred between 1992 and 2015 predominantly had DFM 1000-hour values between roughly 7% and 15%. DFM 1000-hour values have seen significant declines over the past several decades across California and the Western U.S. as a whole due to climate change (Liu 2017; Williams et al. 2019), so a continuing trend would aid in increasing the fire danger in the state. Similar to the top-ranked combination of relative humidity and TKE 50 meters AGL, only 17,871 days were considered in both combinations due to the missing TKE 50 meters AGL data (39 days). As such, 21 out of the 17,871 days

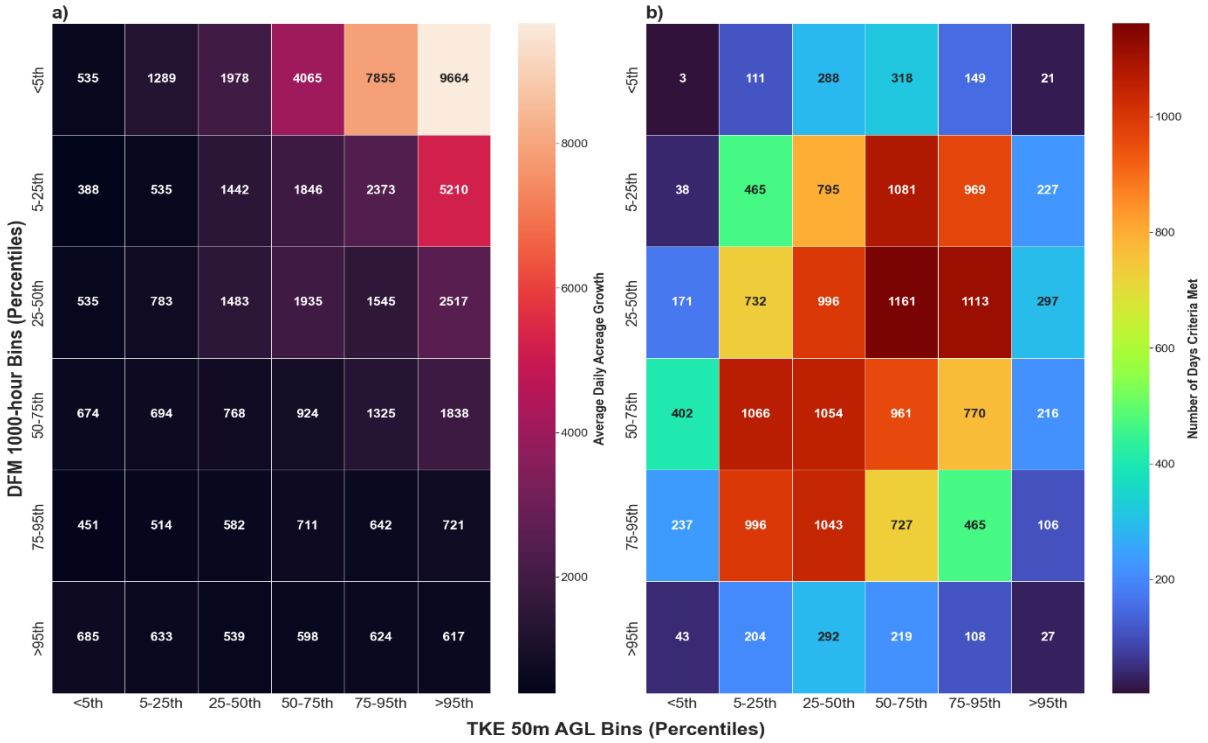

FIG. 5. The heatmap for DFM 1000-hour and TKE 50m AGL. As with Fig. 2, this heatmap converges to the top-right corner (Fig. 5a). This is the second of two top five rankings, and the second of three in the top six, that involve TKE 50m AGL, which suggests that more emphasis should be placed on it when concerning the possibility of a high daily acreage growth rate.

considered met the criteria of the top-right bin for DFM 1000-hour and TKE 50 meters AGL, while 80 of the 17,871 days met the criteria of the top-right bin for vapor pressure and TKE 50 meters AGL. This resulted in a total summed area burned of just under 203,000 and 590,000 acres, respectively. The heatmap for vapor pressure and TKE 50 meters AGL can be seen in Fig. 6.

b. Line plot trends of average daily acreage growth rates

While the heatmaps show how daily average growth depends on the joint conditions of two variables, they also tell another story. The average daily acreage growth rates in each bin do not increase (decrease) in a linear fashion moving towards (away from) the highest growth

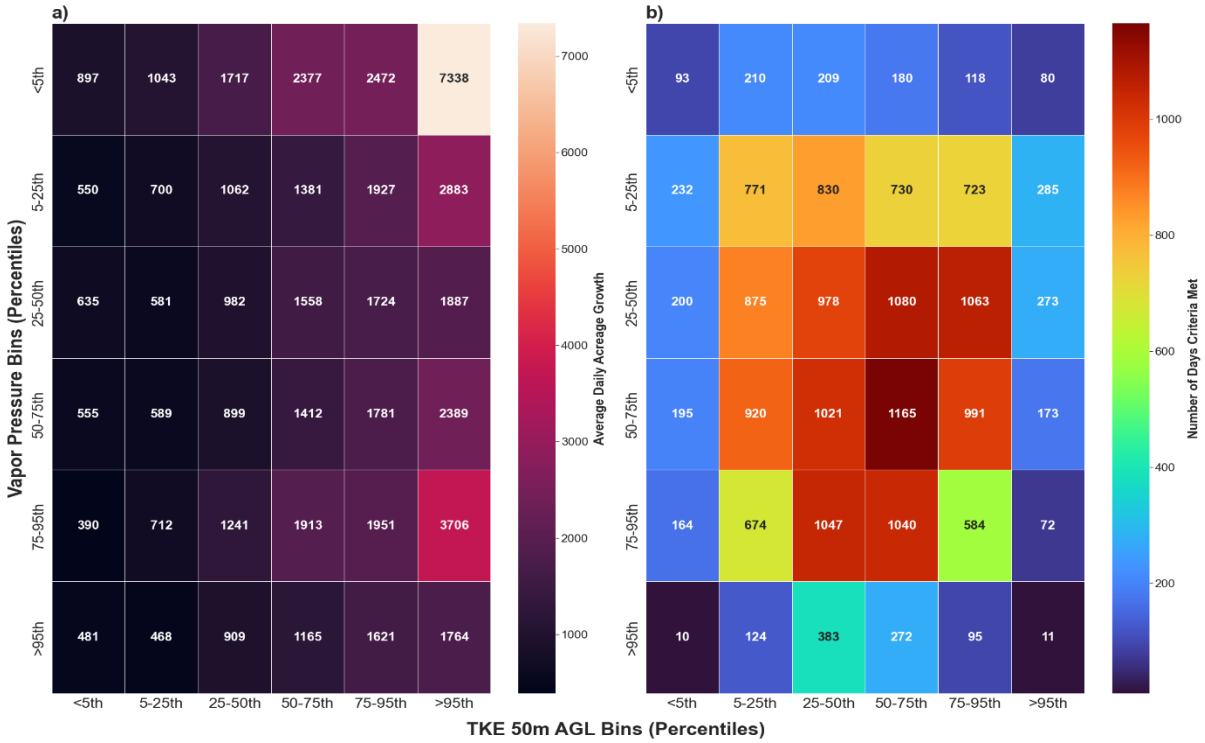

FIG. 6. The heatmap for Vapor Pressure and TKE 50m AGL. As with the other two heatmaps involving TKE 50m AGL, the values converge to the top-right corner (Fig. 6a). This marks the third of six variable combinations in the rankings discussed in this paper that involve TKE 50m AGL.

corner. This indicates that the average daily acreage growth rates are nonlinear and thus increase (decrease) more in accordance with a power law towards (away from) the percentiles associated with high (low) average daily acreage growth. The following figures show these trends (with associated standard errors) for each of the five combinations discussed previously. Each figure contains two plots, with one plot showing the relationships in average daily acreage growth rates for one part of the variable combination as the percentiles increase for the second part of the variable combination. For example, Fig. 7a shows how the average daily acreage growth rates change for all TKE 50m AGL percentile conditions as relative humidity percentile conditions are increased, while Fig. 7b shows the

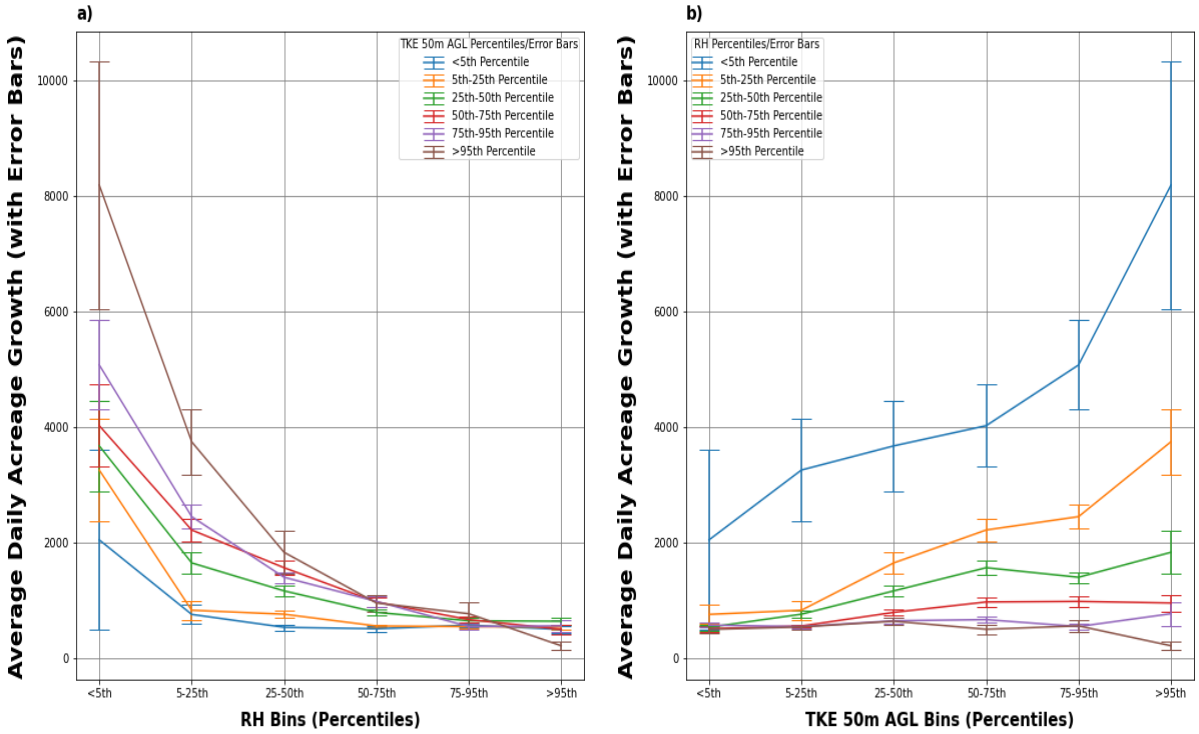

FIG. 7. The Relative Humidity and TKE 50m AGL plot showing the overall trends in average daily acreage growth rates for (a) TKE 50m AGL and (b) Relative Humidity at each percentile of the other variable not plotted. In Fig. 7a, we can clearly see an exponential decrease in average daily acreage growth rates across all TKE 50m AGL percentiles as Relative Humidity conditions move towards the higher percentile conditions (i.e., higher Relative Humidity values). Fig. 7b trends are more linear in nature, but still show dramatic increases in average daily acreage growth rate values across several Relative Humidity percentiles as TKE 50m AGL percentile conditions increase.

same thing, but with the variables reversed. Standard errors are also plotted to indicate the uncertainty for each average daily acreage growth rate value within the plot.

Each plot indicates different relationships; however, there are similarities between the different figures. Fig. 7a, which details the growth rate trends for each of the TKE 50m AGL percentiles as the RH percentile conditions increase, shows a clear power law-like change throughout in average daily acreage growth rates. Fig. 7b, which flips the variables, shows a more linear-like trend; however, there are jumps in the average daily acreage growth rates as the conditions become more conducive for wildfires. The standard errors are quite large in

the more extreme range of conditions in Figs. 7a and 7b, reflecting the smaller number of samples from these conditions. Nevertheless, the figures overall show a clear point where the average daily acreage growth rates are highest and lowest. We find that RH needs to be low enough (below the 25th percentile) for a relationship between TKE and fire growth to emerge. If RH is not low enough, there is no relationship between TKE and fire growth. On the other hand, TKE does not exert the same controls on the relationship between RH and fire growth. No matter how low TKE is, there is still a relationship between RH and fire growth.

Similar results can be seen in Figs. 8 and 9, which detail the trends for the sustained wind speed and DFM 100-hour combination and sustained wind speed and relative humidity combination, respectively. Power law-like decreases (increases) in the average daily acreage growth rates are visible in Figs. 8b and 9b as the percentile conditions for moisture variables plotted in each (Fig. 8b: DFM 100-hour; Fig. 9b: relative humidity) increases (decreases). The trends are more linear in Figs. 8a and 9a, but substantial increases in the average daily acreage growth rates are noted as the percentile conditions increase.

It is also worth mentioning the flatline average daily acreage growth rates seen in the figures discussed so far. For example, in Fig. 8a, the average daily acreage growth rates for DFM 100-hour conditions in the 75th or greater percentiles do not increase even when moving into sustained wind speed conditions more conducive to fire growth, indicating that the available moisture content prohibits large acreage growth rates from being seen. Growth rates like this can be seen in all the figures discussed in this section, showing that while one variable may have extreme conditions that aid in fire growth, the opposing variables' conditions are adequate enough to offset this. This is a particularly interesting finding, as it

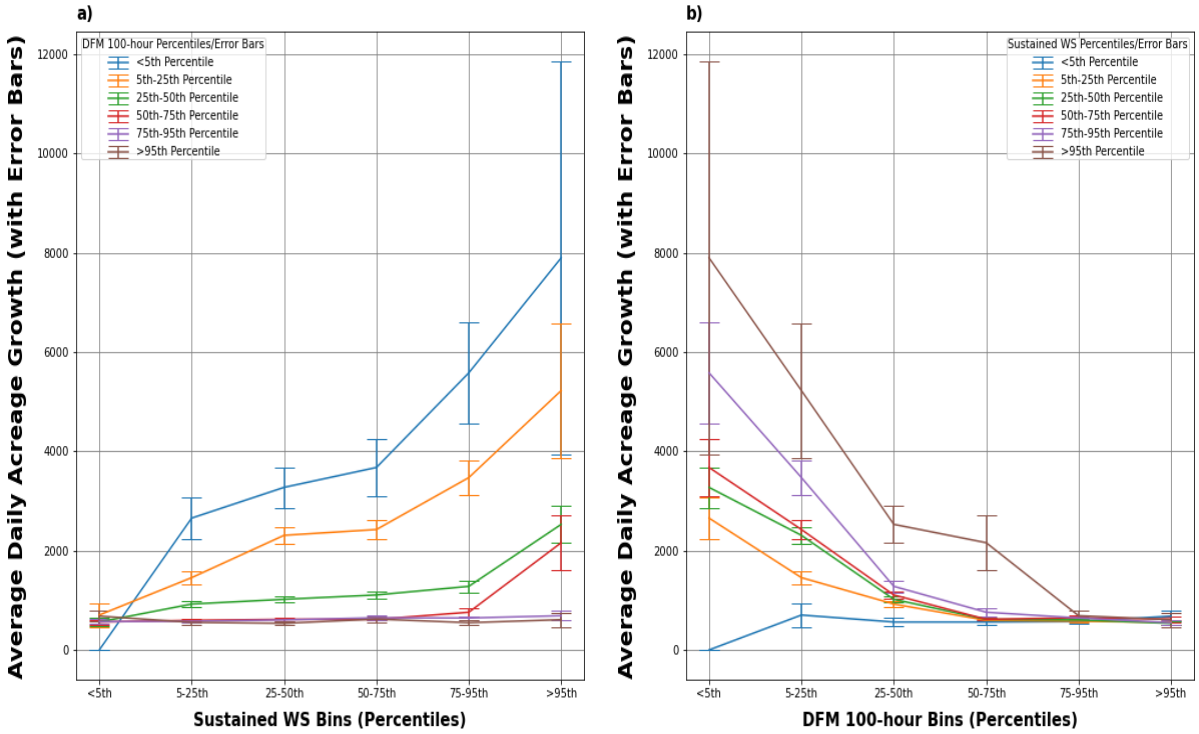

FIG. 8. The plot for the Sustained Wind Speed and DFM 100-hour combination. Fig. 8a details the trends in average daily acreage growth rates for the DFM 100-hour percentile conditions as the Sustained Wind Speed percentile conditions increase, with Fig. 8a showing the daily acreage growth rates for Sustained Wind Speed percentile conditions as DFM 100-hour percentile conditions increase. Similar to Fig. 7, noted large increases in the average daily acreage growth rates at various points in both plots can be seen, indicating nonlinear-like trends in the growth rates as conditions change.

indicates that some variables may play a more important role in determining the likelihood of large acreage growth rates occurring than others. This is a logical explanation; for example, within Fig. 9, the high DFM 100-hour values would serve to counteract the high sustained wind speed values seen concurrently, as fuels that contain more moisture are difficult to ignite. This negates the high sustained wind speeds, as the likelihood of a fire igniting for the sustained wind speeds to fan and increase the size of decrease under wetter fuel conditions.

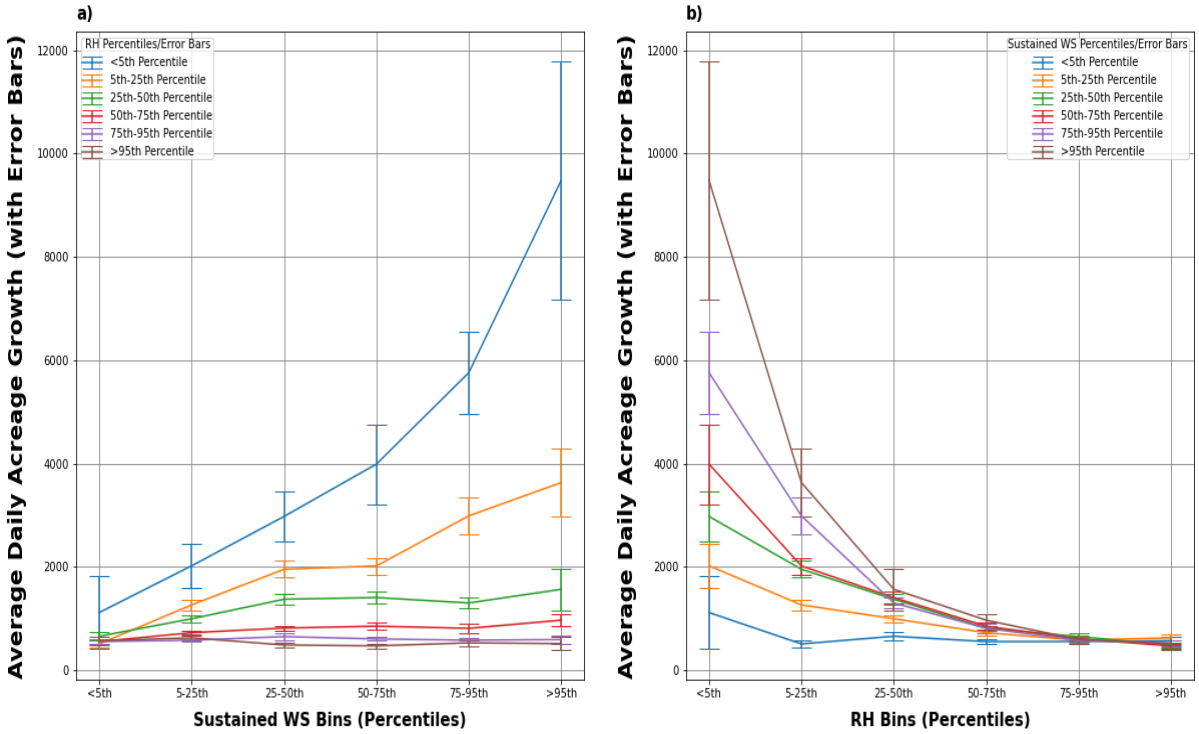

FIG. 9. The plot for the Sustained Wind Speed and Relative Humidity combination. The figure mirrors that of Fig. 8, with Fig 9a showing the average daily acreage growth rate trends for Relative Humidity percentile conditions as Sustained Wind Speed percentile conditions increase. Fig 9b shows the same, but with the variables flipped. Fig. 9b is more exponential-like regarding average daily acreage growth rate trends, but substantial increases can be seen in Fig. 9a in the average daily acreage growth rates as more conducive wildfire conditions occur.

DFM 1000-hour and TKE 50m AGL is shown in Fig. 10. Much like with Fig. 7a, Fig. 10a shows power law-like qualities regarding the decrease (increase) in average daily acreage growth values for the TKE 50m AGL percentile conditions as the DFM 1000-hour percentile conditions increase (decrease), whereas the value changes in Fig. 10b have more linear-like qualities except for the large increases in the higher percentile conditions of DFM 1000-hour as TKE 50m AGL percentile conditions increase, similar to Fig. 7b. Of the line plots shown, the line plot for vapor pressure and TKE 50 meters AGL, shown in Fig. 11, is the most different. In Fig. 11a, most of the average daily acreage growth values for the percentile

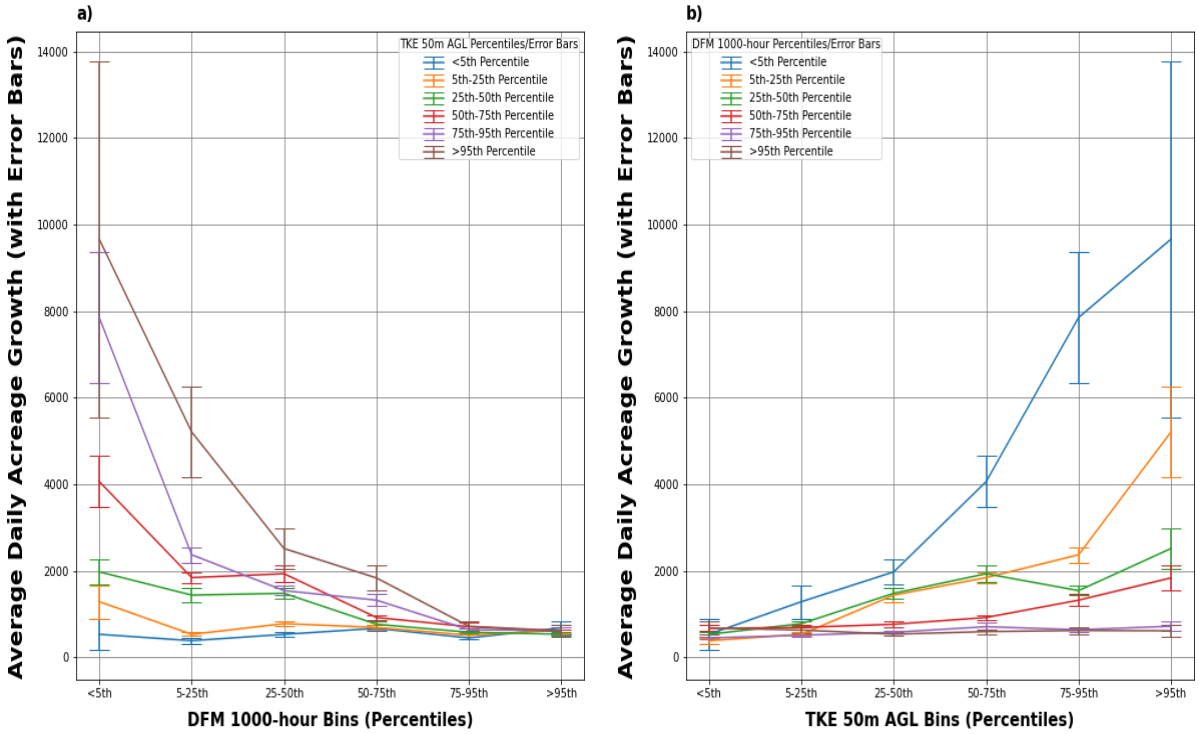

FIG. 10. The plot for the DFM 1000-hour and TKE 50m AGL combination. Fig. 10 is similar to Fig. 7, with Fig. 10a showing a dramatic, exponential-like decrease (increase) in average daily acreage growth for TKE 50m AGL percentile conditions as DFM 1000-hour percentile conditions increase (decrease). Fig. 10b, which is more linear-like than its counterpart in Fig. 10a, still shows non-linear qualities, such as the marked increases (decreases) in average daily acreage growth for DFM 1000-hour percentile conditions as TKE 50m AGL percentile conditions increase (decrease).

conditions of TKE 50m AGL do not change much as the vapor pressure percentile conditions increase or decrease, with the notable exception of the TKE 50m AGL >95th Percentile. Conversely in Fig. 11b, while the average daily acreage growth values of the vapor pressure percentile conditions increase (decrease) as the TKE 50m AGL percentiles increase (decrease), the value changes are virtually uniform throughout most of the vapor pressure percentile conditions except towards the higher TKE 50m AGL percentiles. These differences are important to note. It is likely that the flatline growth seen in Fig. 11a is due to the counterbalance act vapor pressure and TKE 50m AGL play. In Fig. 11b, the slow

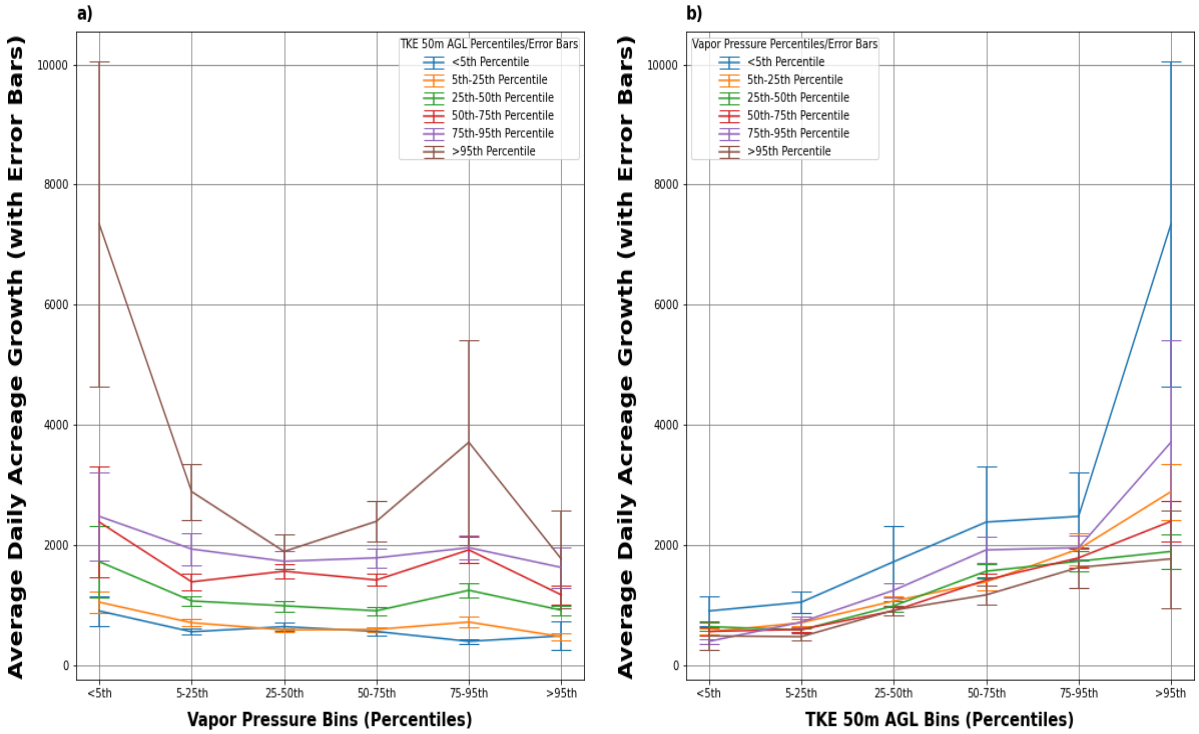

FIG. 11. The plot for the Vapor Pressure and TKE 50m AGL combination. Fig. 11 is more varied than the other plots. Fig. 11a shows flatline average daily acreage growth rates for several of the TKE 50m AGL percentile conditions as Vapor Pressure percentile conditions increase or decrease, with the only main exception being the >95th Percentile for TKE 50m AGL. Fig. 11b, while showing increases (decreases) in average daily acreage growth for Vapor Pressure percentile conditions as TKE 50m AGL percentile conditions increase (decrease), are nearly uniform throughout, with the average daily acreage growth values for the Vapor Pressure percentile conditions increasing at a nearly constant rate throughout all six percentile lines of TKE 50m AGL until the last few percentiles.

increase in the average daily acreage growth values for vapor pressure is almost uniform until the end, when the values see a large jump at the high range of the TKE 50m AGL percentile conditions. This could be attributed to a number of things. The higher range of the vapor pressure percentile values is likely counteracted by the lower range TKE 50m AGL percentile values, until the 50th-75th percentile range of TKE 50m AGL when it appears the TKE 50m AGL values aid in overcoming the high vapor pressure values to produce higher

average daily acreage growth values or increase the average daily acreage growth values together.

c. Corresponding sounding results

Corresponding sounding profiles were created for each bin of the heatmaps. Only the highest acreage growth value corner bin and corresponding opposite corner bin charts will be shown in this paper. While the opposite corner bin might not necessarily have the lowest daily acreage growth value, it allows for a comprehensive look at the conditions seen on days that meet the opposite criteria of the highest daily acreage growth bin days. Each of the soundings is denoted by the variable combination and which corner (highest daily acreage growth, lower daily acreage growth) is plotted in the figure descriptions. As mentioned previously, the vertical profile data was selected for each of the days that met the bin criteria and then averaged. From the averaged data, mean-sounding profiles are plotted. The averaged data also allows for a crude understanding of the mean topographic elevation and the general area within the state the fire days occurred. It should be noted that the daily values themselves - before being averaged - represent the mean daily values, not the values at the daily peak fire growth. Likely because of this and directional cancellation within averaging, wind speed values are lower than they would be if they corresponded to values at the time of largest growth.

The green, red, and black lines on the sounding represent the dewpoint temperature, air temperature, and parcel profile, respectively. Many similarities can be observed throughout both the high- and low-growth corner sounding profiles, indicating general observations that should be looked for on sounding profiles on a forecasted dangerous fire weather day. The

high-growth corner sounding profiles feature large dewpoint depressions, warm-to-hot air temperatures, and high lifted condensation level (LCL) (denoted as the black dot on the sounding) pressure heights. Both the large dewpoint depressions and high LCL pressure heights are indicative of a dry atmospheric environment, which is to be expected on a dangerous fire weather day. Conversely, the low-growth corner sounding profiles reveal cooler, moister environments, with cooler air temperatures, small dewpoint depressions, low LCL pressure heights, and a lack of surface winds being present. As with the high-growth corner sounding profiles, this is expected. Such sounding profiles indicate an atmospheric environment much more hostile to fire growth than its high-growth corner counterparts.

The noted characteristics mentioned above can be clearly seen throughout the sounding profiles. For example, in Fig. 12, representing the relative humidity and TKE 50 meters AGL variable combination, a large dewpoint depression can be seen in Fig. 12a, with a value of near 30°C. Contrarily, in Fig. 12b, the dewpoint depression is much smaller, at only a few degrees Celsius. Similar sights can be seen in the high- and low-growth corner sounding profiles of the other variable combinations. Regarding the sustained wind speed and DFM 100-hour combination (Fig. 13), the dewpoint depression for the high-growth corner sounding profile in Fig. 13a is near 30°C, compared to the much smaller dewpoint depression seen in Fig. 13b in relation to the low-growth corner sounding.

Similarly, the difference between the LCL pressure heights in low- and high-growth corner soundings of the variable combinations is notable. Using the American Meteorological Society's (2012) definition of the LCL, it is the atmospheric level where, when lifted dry-adiabatically, a moist parcel of air becomes saturated. It offers a rough

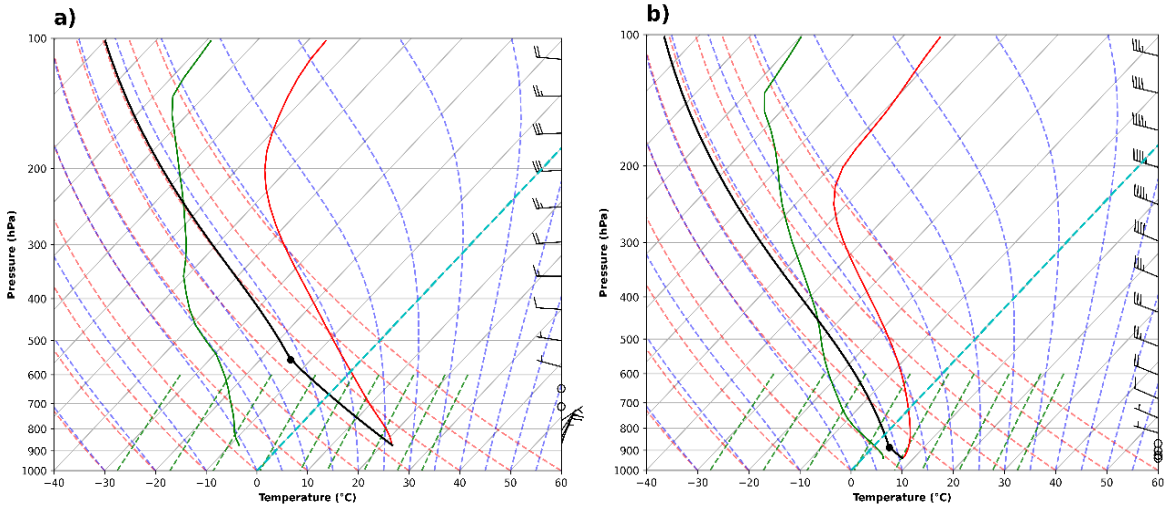

FIG. 12. Skew-T Log P charts for the highest daily acreage growth bin (Fig. 12a) in the Relative Humidity and TKE 50m AGL heatmap and the opposite corner (Fig. 12b) in the heatmap. A large dewpoint depression, high LCL pressure height, warm-to-hot surface temperature, and northeasterly surface winds can be seen in Fig. 12a while a smaller dewpoint depression, lower LCL pressure height, cooler surface temperature, and no surface winds can be seen in Fig. 12b.

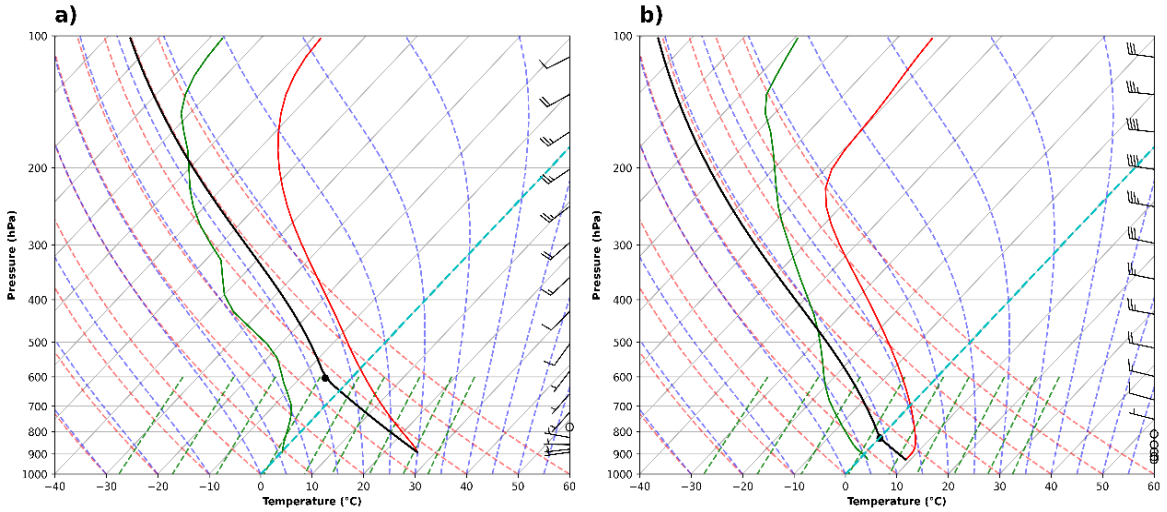

FIG. 13. The soundings for Sustained Wind Speed and DFM 100-hour. Moisture is lacking in the Skew-T Log P chart for the highest daily acreage growth bin (Fig. 13a), which can be seen by the large dewpoint depression and the high LCL pressure height. Conversely, the lower daily acreage growth in (Fig. 13b) has a lower dewpoint depression and LCL pressure height, indicative of more moisture available. Fig. 13a has a warm-to-hot surface temperature and available surface winds (out of the westerly direction), compared to the cooler surface temperature and lack of surface winds seen in Fig. 13b.

estimation of the height of the cloud base. Within the soundings, high-growth corner profiles see LCL pressure heights that are indicative of a dry atmosphere. Fig. 14 denotes the sounding profiles for sustained wind speed and relative humidity. In the high-growth corner sounding profile of Fig. 14a, the LCL pressure height is near 575 hPa, compared to the LCL pressure height of just above 900 hPa seen in the low-growth sounding profile of Fib. 14b. In the sounding profiles for the DFM 1000-hour and TKE 50 meters AGL variable combination (Fig. 15), the LCL pressure heights for the high- and low-growth corner sounding profiles (Fig. 15a and Fig. 15b, respectively) are similar to the other corresponding high-growth corner sounding profiles, with values of near 600 hPa and 800 hPa, respectively.

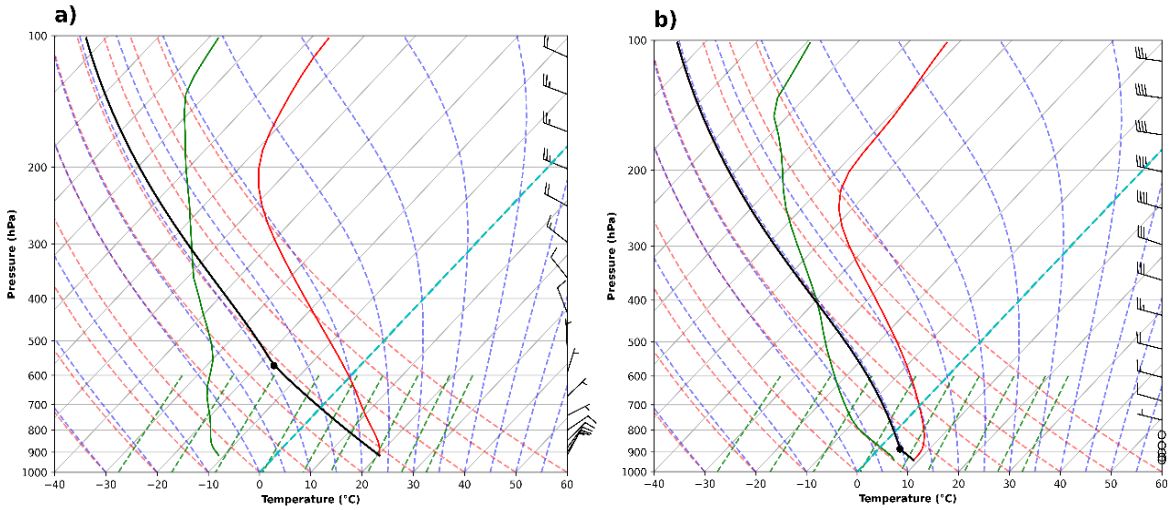

FIG. 14. The soundings for Sustained Wind Speed and Relative Humidity. Note, again, the large dewpoint depressions and large LCL pressure heights in the highest daily acreage growth bin (Fig. 14a), showing a dry environment. Fig. 14b is more moisture laden, with cooler surface air temperatures as well. Surface winds are out of the northeasterly direction in Fig. 14a, with more directional shear throughout the surface- to mid-level areas of the sounding. Conversely, there are no surface winds in the lower daily acreage growth bin chart (Fig. 14b).

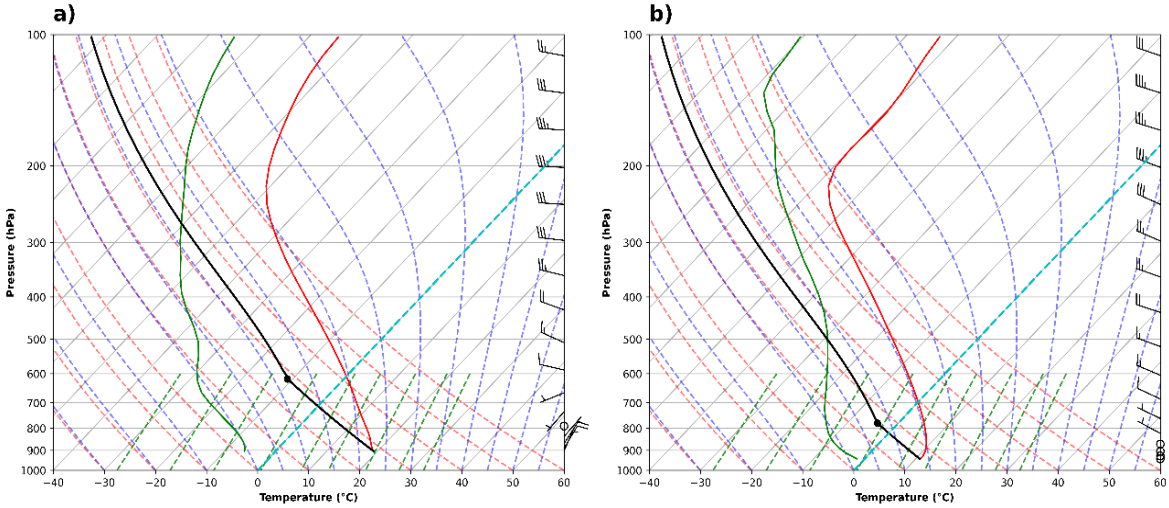

FIG. 15. The soundings for DFM 1000-hour and TKE 50m AGL. As with the other variable combinations, a large dewpoint depression and high LCL pressure height are visible in the chart for the highest daily acreage growth value (Fig. 15a), whereas the dewpoint depression is smaller and LCL pressure height is lower in the chart for the opposite corner (Fig. 15b). Additionally, Fig. 15a has a higher surface air temperature than Fig. 15b, with surface winds out of the northeasterly direction in Fig. 15a and surface winds nonexistent in Fig. 15b.

The surface air and dewpoint temperatures and LCL pressure heights in both the high-growth corner and low-growth corner soundings vary but display the characteristics of high and low acreage growth days described previously. Surface air and dewpoint temperatures present on the high-growth corner sounding profiles range from 20°C to 26°C and -14°C to 0°C, respectively, with the notable exception of the surface air temperature in the high-growth corner sounding profile of the vapor pressure and TKE 50 meters AGL variable combination represented in Fig. 16a. The surface temperature is much lower in this sounding, with a value of just above 10°C; the surface air temperature in the low-growth corner sounding profile presented in Fig. 16b is warmer than that of its high-growth corner sounding counterpart. Even still, the dewpoint depression in Fig. 16a is large, signaling similar characteristics to its counterparts in Figs. 12a-15a. LCL pressure heights throughout

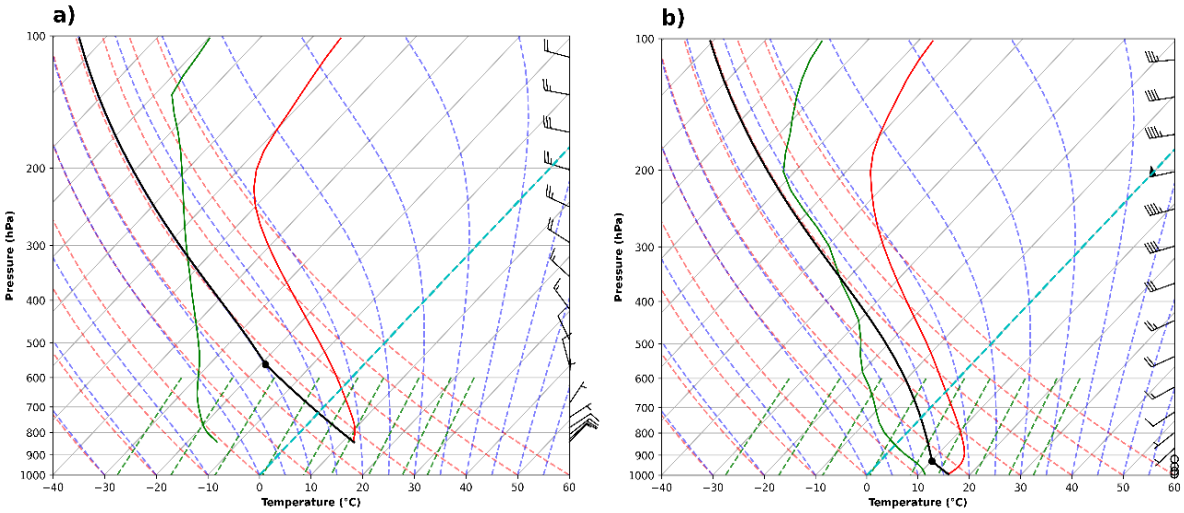

FIG. 16. The soundings for Vapor Pressure and TKE 50m AGL. The consistent large dewpoint depression and high LCL pressure height for high-growth corner soundings are seen in the Vapor Pressure and TKE 50m AGL high-growth corner sounding (Fig. 16a). The dewpoint depression and LCL pressure height for the low-growth corner sounding (Fig. 16b) is much smaller, consistent with the dewpoint depressions and LCL pressure heights seen in Figs. 12b-15b. The air and dewpoint temperatures in the high-growth corner sounding are the lowest among the high-growth corner soundings discussed. This data, along with the northeasterly direction winds at the surface- and low-level areas, indicate a fire environment likely seen in the late fall months when temperatures begin to decrease and wind events such as Diablo or Santa Ana winds are more prevalent.

Figs. 12a-16a range from about 600 millibars to 550 millibars. Again, the resultant dewpoint depression and high LCL pressure heights indicate the overall dryness of the atmospheric profile. Regarding the low-growth corner soundings, the surface air and dewpoint temperatures range from 8°C to 15°C and -2°C to 11°C, respectively, with LCL pressure heights ranging from 920 millibars to 780 millibars, showing the overall cool, moisture-laden atmospheric profiles present during fire days that see little or no growth.

While there are several similarities between the high-growth corner soundings, one major difference is noticeable: the wind profile of the soundings. The surface to low-level winds on four of the high-growth corner sounding profiles (Figs. 12a, 14a-16a) differ from the other (Fig. 13a), suggesting different wind regimes that may play a role in aiding fire growth. In

Figs. 12a and 14a-16a, the winds are out of the northeasterly direction. Conversely, in Fig. 13a, the surface winds are out of the westerly direction. The northeasterly directional surface winds would be indicative of either Santa Ana or Diablo winds. Considering this and some of the cooler range of air temperatures in the high growth sounding profiles described previously (most exemplified by Fig. 16a), it is likely that some of the sounding profiles characterize what is typically seen during a Diablo wind event, as Diablo winds are known to be generally northeasterly winds and have been found to not have associated daily maximum and minimum temperatures above climatological values (Smith et al. 2018). Similar to the surface winds, there are also differences between the high-growth sounding profiles mid- and upper-level winds, with Fig. 13a having southwesterly winds above 700 millibars while the other four high-growth corner soundings have more westerly winds. Pronounced directional shear is present throughout much of the wind profile from the surface to mid-levels before diminishing as the pressure decreases. This is perhaps the biggest difference between the high-growth corner profiles, as the pressure at which directional shear decreases varies throughout all five profiles, becoming more unidirectional anywhere from 700 millibars to 300 millibars. Regarding wind speeds, the surface to low-level winds are less than five knots while the mid- to upper-level wind speeds are generally in the range of 10 knots to 20 knots, with the low wind speed values being attributed to the reasons discussed in the first paragraph of this section.

Conversely, the wind profiles on the low-growth corner sounding profiles are virtually similar throughout, with only minor differences. Throughout the soundings (Figs. 12b-16b), a lack of surface to low-level winds can be seen. Mid- to upper-level winds have variations in

speeds but remain, generally, out of the westerly direction throughout the five soundings. Mid- to upper-level wind speeds are more varied in each of the soundings compared to those seen in the high-growth corner profile soundings, with Fig. 16b, for example, ranging from 10 knots to 50 knots throughout the wind profile.

The sounding profiles are useful in giving an inside look at the average atmospheric conditions seen for each bin in each heatmap. It should be noted, again, that the overall wind profiles of the soundings show weak winds at various points throughout the sounding profiles. As mentioned previously, this is likely because the datasets represent daily averaged values, thus the averaged wind speed values will be lower as the highest wind speeds only occurred over a small time period. It is also likely due to directional cancellation within the averaging. All of the u- and v-wind values are averaged together, but, for example, u-wind values of -6, -4, 3, and 7 would average to 0, thus giving a value that is lower than what is likely seen on an average day that meet the criteria. Large dewpoint depressions and high LCL pressure heights being commonplace in the highest daily acreage growth bins is not surprising, as these characteristics are indicative of a dry atmosphere, which, along with warm to hot surface temperatures, is a characteristic of wildfire days (Dong et al. 2021). This can be correlated to the Haines Index, as Winkler et al. (2007) found the 1961 to 2000 average 700 millibar dewpoint depressions in excess of 20°C over much of the state, corresponding to the maximum value of the Haines Index moisture component (B). The difference in surface wind direction throughout the various sounding profiles shown is noteworthy, though. Northeasterly surface winds are perhaps indicative of Diablo or Santa Ana wind events occurring, which would validate the emphasis placed on both during the

wildfire season as key components to use regarding the potential for dangerous fire weather days. Low-growth corner profiles showing a moister, cooler environment with a lack of surface winds should not be surprising, as those components indicate a more hostile environment for fire growth.

4. Summary and Conclusions

Sustained wind speed and relative humidity are widely used to discern fire weather danger. This study uses high-resolution historical reanalysis combined with satellite fire growth data to assess the empirical effectiveness of relative humidity and sustained wind speed in representing conditions conducive to large fire growth and to determine if more viable variable combinations (17 variables, 136 total combinations) exist that could be used to create a new warning index that more accurately predicts high acreage growth rates. Our approach was to separate variable values into bins corresponding to specific percentile ranges (<5th Percentile, 5th-25th Percentile, 25-50th Percentile, 50th-75th Percentile, 75th-95th Percentile, >95th Percentile) and make joint distributions of fire growth (heat maps) for all pairwise variable combinations. We investigate the top five ranked heatmaps in detail and supplement the analysis with investigations of the changes in average daily acreage growth rates as variable percentile values change and the vertical profiles of temperature, moisture, and wind.

In confirmation of conventional wisdom, our data suggest that sustained wind speed and relative humidity are indeed very useful for describing conditions conducive to large growth; however, two variable combinations - relative humidity and TKE 50m AGL and sustained wind speed and DFM 100-hour - are ranked the highest using the ranking system devised. Sustained wind speed and relative humidity placed in a tie for third in the rankings, indicating its strong usefulness in predicting and describing fire danger potential. TKE 50m AGL and DFM 1000-hour and vapor pressure and TKE 50m AGL rounded out the rankings discussed in a tie for fifth. Sustained wind speed and DFM 1000-hour tied with sustained

wind speed and relative humidity; however, their exclusion from discussion here was due to the physical and visual similarities with sustained wind speed and DFM 100-hour. Though relative humidity is included in two of the top four rankings, DFM being involved in half of the top six rankings suggests it might be more useful than relative humidity. Relative humidity is a diurnal variable, whereas DFM 100- and 1000-hour values change more slowly. Thus, relative humidity values might not necessarily denote an accurate representation of the environmental moisture conditions present on a given day.

While the inclusion of relative humidity and sustained wind speed in the top five rankings is expected, TKE 50m AGL being a part of the top variable combination overall in the rankings is noteworthy. Its effects on wildfires have been noted, however, by Heilman and Bian (2010), finding that high near-surface TKE values are associated with strong wind gusts and variable wind regimes at the surface. Furthermore, TKE captures the gusty wind speeds seen near the surface at a high frequency and at a higher resolution than sustained wind speed. Considering this and the findings of this study, TKE could make for a logical variable to use in the creation of fire weather forecasts. Its inclusion in three of the top five rankings discussed was not expected, however. This underlines the potential importance of TKE regarding fire weather forecasts.

Aside from TKE, the other variables involved in the top five rankings - sustained wind speed, relative humidity, and DFM 100- and 1000-hour - are understandable. Emphasis has always been placed on moisture variables regarding fire weather danger, but more may be needed as fuel aridity continues to increase and fire season becomes longer (Abatzoglou and Williams 2016). However, a main conclusion drawn from this study is that the traditional

variables used when issuing RFWs are validated with the empirical data. While several variable combinations were found to perform better than or close to sustained wind speed and relative humidity, the limited public knowledge of terms like TKE and fuel moisture content could prevent wildfire information from being easily understood by the general public. That said, the findings regarding TKE 50m AGL should be strongly considered, as the underlying variables used to create fire weather forecasts do not rely on an understanding on part of the general public.

The results of the averaged sounding profiles created for each high-growth and low-growth corner of the variable rankings discussed are expected. Overall, the high-growth corner soundings were accompanied by high LCL pressure heights and large dewpoint depressions, indicative of a very dry atmosphere. Coupled with wind regimes typical of California (i.e., Diablo and Santa Ana winds) that aid in the growth of fires, the soundings produced paint a very explosive picture regarding the potential for fire growth. Conversely, the soundings of the low-growth corners are moister and cooler generally, thus leading to inhibiting conditions for fire growth. It is worth noting the presence of cooler surface temperatures on high acreage growth days that are coupled with northeasterly surface winds, as this could represent atmospheric environments associated with Diablo wind events. Work done by Smith et al. (2018) supports this finding.

Regarding the line plots produced that show the average daily acreage growth values as percentile values for each variable are increased or decreased, the results are interesting. The line plots show a general nonlinearity trend in the average daily acreage growth values moving from bin combination to bin combination. This shows that there is no linear increase

in the area burned or the size of wildfires within the state as values for the variable combinations shown increase or decrease. It emphasizes the unpredictability of growth rate or area burned under specific conditions, while also showing the dangers associated with compound extreme conditions (multiple variables being in extreme states simultaneously) and how growth rate and area burned can rapidly increase during these said conditions. Additionally, the presence of flatline growth in several of the line plots suggests that the dangerous effects of certain variables can be negated by values of other variables not associated with high average daily acreage growth.

Much of the rankings were not discussed in this paper; however, the overall rankings are still worth briefly mentioning. Of the 136 different variable combinations considered, there were several surprises regarding the lower ranked variable combinations. For instance, a variable combination involving the Haines Index did not place higher than a tie for 13th in the overall rankings, with 8 of the possible 16 different variable combinations placing in the bottom half of the rankings. Considering that the Haines Index is a specific derived value meant to represent fire danger, this is surprising. However, the reliability and added forecasting benefit of the Haines Index has been researched and scrutinized by several voices within the wildfire community (Potter 2018; Srock et al. 2018). The lack of predictive power associated with the Haines Index in this study supports those criticisms. Elsewhere, another surprising result was the performance of VPD compared to relative humidity. 5 of the 16 possible combinations involving relative humidity placed in the top 10 rankings, compared to none involving VPD. 12 of the 16 possible combinations involving relative humidity were ranked in the top half of the rankings, compared to 10 of 16 combinations involving VPD.

Additionally, 6 of the combinations involving VPD ranked in the bottom third of the rankings, with only 2 of the combinations involving relative humidity placing in that same category. Lastly, given the good performance overall of DFM 100-hour and TKE, it is a surprise that that variable combination placed near the exact middle of the rankings, in a tie for 63rd. One would think that the variable combination would place higher. More research on the physical mechanisms underlying these rankings should be undertaken in the future.

This study does have its limitations. The figures generated considered all vegetation fuel types, disregarding the location the wildfires in the dataset occurred. It is essential for future research to separate the fires by land use, revealing important differences in relationships between fires in different fire regimes. Variable combination rankings may differ for each land use type (forest, shrub, and savanna and grassland), thus leading to different variable combinations that could be used in different ecoregions of the state to help predict large acreage growth days. Additionally, the dataset used was geographically restricted to central and northern portions of the state of California, so it is unknown if these findings generalize to other regions. Like with land use type, different variable combination rankings from the ones discussed in this paper may exist for other locations. More research into both of these areas could be done including extending the geographic area to include the Pacific Northwest, the Intermountain region, and the Desert Southwest.

Climate change continues to worsen the wildfire season in California. Northern portions of the state have been particularly hit hard, with increases of over 600% in annual area burned seen in the North Coast and the Sierra Nevada regions (Williams et al. 2019). Aside from 2019, every fire season since 2017 has seen over one and a half million acres burned in

the state, with a staggering four million acres burned in 2020 alone (CALFIRE 2022b). Increased wildfire activity increases the importance of wildfire forecasting. Being able to better predict large acreage fire growth will aid substantially in preparing the public. Federal, state, and local resources will also be better positioned to mitigate the impact of these large acreage fires. While this study confirms the utility of variables already in widespread use, it also sheds new light on their relationships with wildfire danger, highlighting for example, nonlinearities when multiple variables, in their extreme state, act together to increase the wildfire potential.

References

Abatzoglou, J. T., and C. A. Kolden, 2013: Relationships between climate and macroscale area burned in the western United States. *Int. J. Wildl. Fire*, **22**, 1003–1020, https://doi.org/10.1071/WF13019.

——, and A. P. Williams, 2016: Impact of anthropogenic climate change on wildfire across western US forests. *Proc. Natl. Acad. Sci. U. S. A.*, **113**, 11770–11775, https://doi.org/10.1073/pnas.1607171113.

——, J. K. Balch, B. A. Bradley, and C. A. Kolden, 2018: Human-related ignitions concurrent with high winds promote large wildfires across the USA. *Int. J. Wildl. Fire*, **27**, 377–386, https://doi.org/10.1071/WF17149.

——, D. S. Battisti, A. P. Williams, W. D. Hansen, B. J. Harvey, and C. A. Kolden, 2021: Projected increases in western US forest fire despite growing fuel constraints. *Commun. Earth Environ.*, **2**, 227, https://doi.org/10.1038/s43247-021-00299-0.

American Meteorological Society, 2012: Lifting condensation level. Accessed 7 December 2022, https://glossary.ametsoc.org/wiki/Lifting_condensation_level.

Brey, S. J., E. A. Barnes, J. R. Pierce, C. Wiedinmyer, and E. V. Fischer, 2018: Environmental conditions, ignition type, and air quality impacts of wildfires in the southeastern and western United States. *Earth's Futur.*, **6**, 1442–1456, https://doi.org/10.1029/2018EF000972.

CALFIRE, 2022a: Camp fire incident. Accessed 8 August 2022, https://www.fire.ca.gov/incidents/2018/11/8/camp-fire/.

——, 2022b: Stats and events. Accessed 8 June 2022, https://www.fire.ca.gov/stats-events/.

——, 2022c: Top 20 largest California wildfires. Accessed 31 May 2022, https://www.fire.ca.gov/media/4jandlhh/top20_acres.pdf.

——, 2022d: Top 20 most destructive California wildfires. Accessed 8 August 2022, https://www.fire.ca.gov/media/t1rdhizr/top20_destruction.pdf.

Clark, J., J. T. Abatzoglou, N. J. Nauslar, and A. M. S. Smith, 2020: Verification of red flag warnings across the northwestern U.S. as forecasts of large fire occurrence. *Fire*, **3**, 1–17, https://doi.org/10.3390/fire3040060.

Dong, L., L. R. Leung, Y. Qian, Y. Zou, F. Song, and X. Chen, 2021: Meteorological environments associated with California wildfires and their potential roles in wildfire changes during 1984–2017. *J. Geophys. Res. Atmos.*, **126**, 1–20, https://doi.org/10.1029/2020JD033180.

Ellis, T. M., D. M. J. S. Bowman, P. Jain, M. D. Flannigan, and G. J. Williamson, 2022: Global increase in wildfire risk due to climate-driven declines in fuel moisture. *Glob. Change Biol.*, **28**, 1544-1559, https://doi.org/10.1111/gcb.16006.

Estes, B. L., E. E. Knapp, C. N. Skinner, J. D. Miller, and H. K. Preisler, 2017: Factors influencing fire severity under moderate burning conditions in the Klamath Mountains, northern California, USA. *Ecosphere*, **8**, e01794, https://doi.org/10.1002/ecs2.1794.

Flannigan, M. D., B. M. Wotton, G. A. Marshall, W. J. de Groot, J. Johnston, N. Jurko, and A. S. Cantin, 2016: Fuel moisture sensitivity to temperature and precipitation: climate change implications. *Clim. Change*, **134**, 59–71, https://doi.org/10.1007/s10584-015-1521-0.

Gergel, D. R., B. Nijssen, J. T. Abatzoglou, D. P. Lettenmaier, and M. R. Stumbaugh, 2017: Effects of climate change on snowpack and fire potential in the western USA. *Clim. Change*, **141**, 287–299, https://doi.org/10.1007/s10584-017-1899-y.

Goss, M., D. L. Swain, J. T. Abatzoglou, A. Sarhadi, C. A. Kolden, A. P. Williams, and N. S. Diffenbaugh, 2020: Climate change is increasing the likelihood of extreme autumn wildfire conditions across California. *Environ. Res. Lett.*, **15**, 094016, https://doi.org/10.1088/1748-9326/ab83a7.

Heilman, W. E., and X. Bian, 2010: Turbulent kinetic energy during wildfires in the north central and north-eastern US. *Int. J. Wildl. Fire*, **19**, 346–363, https://doi.org/10.1071/WF08076.

Jain, P., D. Castellanos-Acuna, S. C. P. Coogan, J. T. Abatzoglou, and M. D. Flannigan, 2022: Observed increases in extreme fire weather driven by atmospheric humidity and temperature. *Nat. Clim. Chang.*, **12**, 63–70, https://doi.org/10.1038/s41558-021-01224-1.

Jolly, W. M., M. A. Cochrane, P. H. Freeborn, Z. A. Holden, T. J. Brown, G. J. Williamson, and D. M. J. S. Bowman, 2015: Climate-induced variations in global wildfire danger from 1979 to 2013. *Nat. Commun.*, **6**, 1-11, https://doi.org/10.1038/ncomms8537.

Keeley, J. E., and A. D. Syphard, 2019: Twenty-first century California, USA, wildfires: Fuel-dominated vs. wind-dominated fires. Fire Ecology, 15, 24, https://doi.org/10.1186/s42408-019-0041-0.

Kitzberger, T., D. A. Falk, A. L. Westerling, and T. W. Swetnam, 2017: Direct and indirect climate controls predict heterogeneous early-mid 21st century wildfire burned area across western and boreal North America. *PLoS One*, **12**, e0188486, https://doi.org/10.1371/journal.pone.0188486.

Kramer, H. A., M. H. Mockrin, P. M. Alexandre, and V. C. Radeloff, 2019: High wildfire damage in interface communities in California. *Int. J. Wildl. Fire*, **28**, 641–650, https://doi.org/10.1071/WF18108.

Liu, Y., 2017: Responses of dead forest fuel moisture to climate change. *Ecohydrology*, **10**, 1–10, https://doi.org/10.1002/eco.1760.

Ma, W., and Coauthors, 2021: Assessing climate change impacts on live fuel moisture and wildfire risk using a hydrodynamic vegetation model. *Biogeosciences*, **18**, 4005-4020, https://doi.org/10.5194/bg-18-4005-2021.

Martinuzzi, S., S. I. Stewart, D. P. Helmers, M. H. Mockrin, R. B. Hammer, and V. C. Radeloff, 2015: *The 2010 wildland-urban interface of the conterminous United States* [Research Map NRS-8]. U.S. Department of Agriculture, Forest Service, Northern Research Station, 124 pp. https://doi.org/10.2737/NRS-RMAP-8.

Potter, B. E., 2018: The Haines index-It's time to revise it or replace it. *Int. J. Wildl. Fire*, **29**, 437-400, https://doi.org/10.1071/WF18015.

——, and D. McEvoy, 2021: Weather factors associated with extremely large fires and fire growth days. *Earth Interact.*, **25**, 160–176, https://doi.org/10.1175/EI-D-21-0008.1.

Reilly, M. J., M. G. McCord, S. M. Brandt, K. P. Linowksi, R. J. Butz, and E. S. Jules, 2020: Repeated, high-severity wildfire catalyzes invasion of non-native plant species in forests of the Klamath Mountains, northern California, USA. *Biol. Invasions*, **22**, 1821-1828, https://doi.org/10.1007/s10530-020-02227-3.

Smith, C., B. J. Hatchett, and M. Kaplan, 2018: A surface observation based climatology of diablo-like winds in California's wine country and Western Sierra Nevada. *Fire*, **1**, 1–9, https://doi.org/10.3390/fire1020025.

Seager, R., A. Hooks, A. P. Williams, B. Cook, J. Nakamura, and N. Henderson, 2015: Climatology, variability, and trends in the U.S. vapor pressure deficit, an important fire-related meteorological quantity. *J. Appl. Meteorol. Climatol.*, **54**, 1121-1141, https://doi.org/10.1175/JAMC-D-14-0321.1.

Srock, A. F., J. J. Charney, B. E. Potter, and S. L. Goodrick, 2018: The hot-dry-windy index: A new fire weather index. *Atmosphere*, **9**, 1-11, https://doi.org/10.3390/atmos9070279.

Theobald, D. M., and W. H. Romme, 2007: Expansion of the US wildland-urban interface. *Landsc. Urban Plan.*, **83**, 340-354, https://doi.org/10.1016/j.landurbplan.2007.06.002.

Weber, K. T., and R. Yadav, 2020: Spatiotemporal trends in wildfires across the western United States (1950-2019). *Remote Sens.*, **12**, 2959, https://doi.org/10.3390/rs12182959.

Williams, A. P., and Coauthors, 2015: Correlations between components of the water balance and burned area reveal new insights for predicting forest fire area in the southwest United States. *Int. J. Wildl. Fire*, **24**, 14–26, https://doi.org/10.1071/WF14023.

——, J. T. Abatzoglou, A. Gershunov, J. Guzman-Morales, D. A. Bishop, J. K. Balch, and D. P. Lettenmaier2019: Observed impacts of anthropogenic climate change on wildfire in California. *Earth's Future*, **7**, 892–910, https://doi.org/10.1029/2019EF001210.

Winkler, J. A., B. E. Potter, D. F. Wilhelm, R. P. Shadbolt, K. Piromsopa, and X. Bian, 2007: Climatological and statistical characteristics of the Haines Index for North America. *Int. J. Wildl. Fire*, **16**, 139–152, https://doi.org/10.1071/WF06086.

Yuan, W., and Coauthors, 2019: Increased atmospheric vapor pressure deficit reduces global vegetation growth. *Sci. Adv.*, **5**, 1-13, https://doi.org/10.1126/sciadv.aax1396.

Yue, X., L. J. Mickley, and J. A. Logan, 2014: Projection of wildfire activity in southern California in the mid-twenty-first century. *Clim. Dyn.*, **43**, 1973–1991, https://doi.org/10.1007/s00382-013-2022-3.